A new path to platelet production through matrix sensing

by Vittorio Abbonante, Christian Andrea Di Buduo, Cristian Gruppi, Carmelo De Maria, Elise Spedden, Aurora De Acutis, Cristian Staii, Mario Raspanti, Giovanni Vozzi, David Kaplan, Francesco Moccia, Katya Ravid, and Alessandra Balduini

Haematologica 2017 [Epub ahead of print]

Citation: Abbonante V, Di Buduo CA, Gruppi C, De Maria C, Spedden E, De Acutis A, Staii C, Raspanti M, Vozzi G, Kaplan D, Moccia F, Ravid K, and Balduini A. A new path to platelet production through matrix sensing. Haematologica. 2017; 102:xxx
doi:10.3324/haematol.2016.161562

Title: A new path to platelet production through matrix sensing

Authors: Vittorio Abbonante[1,2], Christian Andrea Di Buduo[1,2], Cristian Gruppi[1,2], Carmelo De Maria[3], Elise Spedden[4], Aurora De Acutis[3], Cristian Staii[4], Mario Raspanti[5], Giovanni Vozzi[3], David Kaplan[6], Francesco Moccia[7], Katya Ravid[8], Alessandra Balduini[1,2,6*]

Affiliations:

[1]Department of Molecular Medicine, University of Pavia, Pavia, Italy

[2]Laboratory of Biotechnology, IRCCS San Matteo Foundation, Pavia, Italy

[3]Interdepartmental Research Center "E. Piaggio", University of Pisa, Italy

[4]Department of Physics and Astronomy, Tufts University, Medford, MA, USA

[5]Department of Surgical and Morphological Sciences, University of Insubria, Varese, Italy

[6]Department of Biomedical Engineering, Tufts University, Medford, MA, USA

[7]Department of Biology and Biotechnology "Lazzaro Spallanzani", University of Pavia, Pavia, Italy

[8]Departments of Medicine and of Biochemistry, Boston University School of Medicine, Boston, MA, USA

Running Heads: TRPV4 regulates proplatelet formation

***Alessandra Balduini (alessandra.balduini@unipv.it), Laboratory of Biotechnology, Department of Molecular Medicine, University of Pavia, IRCCS San Matteo Foundation, viale Forlanini 6, 27100 Pavia, Italy. Department of Biomedical Engineering, Tufts University, 4 Colby Street, Medford, MA 02155, USA. Phone +39 0382 502968.

Text word count: 3787

Abstract word count: 165

8 Figures

References: 62

Category: Hematopoiesis

Aknowledgements

We thank Prof. Giampaolo Merlini for providing instruments for polarized light microscopy imaging, Prof. Elisabetta Dejana for helping in setting experiments for integrin internalization, Dr. Manuela Monti for providing instruments for confocal imaging, Dr. Franco Tanzi for providing instruments for calcium imaging, Dr. Jandrot Perrus for providing anti-GPVI antibody. **Funding:** VA fellowship was funded by Collegio Ghislieri, Pavia progetto “Progressi in Biologia e Medicina”. This paper was supported by Cariplo Foundation (2013-0717), US National Institutes of Health (grant EB016041-01) to DK and AB and NHLBI HL80442 to KR. The funders had no role in study design, data collection and analysis, decision to publish, or preparation of the manuscript.

Abstract

Megakaryocytes in the bone marrow are immersed in a network of extracellular matrix components that regulates platelet release into the circulation. Combining biological and bioengineering approaches, we found that the activation of transient receptor potential cation channel subfamily V member 4, a mechano-sensitive ion channel, is induced upon megakaryocyte adhesion on softer matrices. This response promoted platelet production by triggering a cascade of events that lead to calcium influx, β1 integrin activation and internalization, and Akt phosphorylation, responses not found on stiffer matrices. Lysyl oxidase is a physiological modulator of bone marrow matrix stiffness via collagen cross-linking. *In vivo* inhibition of lysyl oxidase and consequent matrix softening lead to transient receptor potential cation channel subfamily V member 4 activation cascade and increased platelet levels. Concurrently, *in vitro* proplatelet formation was reduced on a recombinant enzyme-mediated stiffer collagen. These results suggest a novel mechanism by which megakaryocytes, through transient receptor potential cation channel subfamily V member 4, sense extracellular matrix environmental rigidity and release platelets accordingly.

Introduction

Megakaryocytes (Mks) reside within the bone marrow (BM), where they mature to extend proplatelets, at the end of which newly formed platelets are assembled and released into the bloodstream [1-4]. Different extracellular matrix components (ECM), in the BM, actively regulate megakaryopoiesis[5-7]. In earlier studies, it was demonstrated that type IV collagen sustains proplatelet formation (PPF), opposite to type I collagen, which is a fundamental negative regulator of PPF through integrin α2β1/Rho/ROCK axis engagement [8-12]. In addition, recent studies highlighted the direct involvement of PI3K/Akt and MAPK/ERK pathways in PPF [13-17]. Interestingly, ECM component stiffness was shown to be inversely correlated to Mk maturation and PPF[8,10,18].

Cell contact with ECM components occurs through integrins which transduce the signals from the ECM to the cell cytoskeleton[19-21]. However, to sense the extracellular environment, integrins act in concert with different mechano-sensitive ion channels [22,23]. Among these, the transient receptor potential cation channel subfamily V member 4 (TRPV4) is a membrane mechano-sensitive ion channel whose activation has been linked to activation of β1 integrin a major collagen-binding integrin receptor subunit [24-26]. Interestingly, TRPV4 activity has been demonstrated to modulate PI3K/Akt and MAPK/ERK pathways in endothelial cells upon physical stimuli applied to the cell membrane [24]. In the current study, we demonstrate a new mechanism by which Mks sense the environmental mechanics to regulate their maturation and platelet production. On soft collagenous substrates, TRPV4 expressed on the Mk surface was activated, inducing calcium influx, β1 integrin activation and internalization, with consequent Akt phosphorylation and proplatelet formation.

Methods

In vitro megakaryocyte cultures

Human $CD34^+$ cells were isolated, separated and cultured, as described previously [27,28]. All human samples were collected in accordance with the ethical committee of the IRCCS Policlinico San Matteo Foundation and the principles of the Declaration of Helsinki. For collagen receptor inhibition, Mks at day 13 of culture were incubated with 10 µg/mL anti-β1 integrin blocking

antibody (Millipore, clone P5D2), 10 µg/mL anti-GPVI blocking antibody (a kind gift of Prof. Jandrot Perrus) or with 200 nM (125 ng/mL) Discoidin Domain Receptor 1 (DDR1) -IN-1 (Tocris), a selective DDR1 tyrosine kinase inhibitor, for one hour prior to be plated on type I or type IV collagen for 3 hours. For Akt inhibition experiments, Mks at day 13 of culture were treated with 10 µM Akt1/2 inhibitor (Sigma Aldrich) for 30 minutes and then plated on collagens for 16 hours for PPT evaluation. For treatment with the TRPV4 inhibitors (RN-1734, HC067047, Sigma Aldrich) Mks at day 13 of culture were incubated with vehicle or 10 µM of the indicated TRPV4 inhibitor for 30 minutes prior to be plated on collagens for 3 or 16 hours. For treatment with the TRPV4 agonist (GSK1016790A, Sigma Aldrich), Mks at day 13 of culture were incubated or not with 10 nM GSK1016790A for 10 minutes prior to be plated on collagens for 3 hours.

Evaluation of megakaryocyte spreading and proplatelet formation

Evaluation of Mk spreading and proplatelet formation (PPF) onto collagens was performed as previously described [29]. Please refer to Supplemental Methods for technical details.

Immunoprecipitation and Western blotting

For immunoprecipitation and western blotting analysis, cultured Mks and primary BM immunomagnetically-sorted Mks (CD41+; Biolegend) were collected, washed twice at 4°C and lysed as previously described [30]. For active β1 integrin staining, samples were not reduced. Please refer to Supplemental Methods for technical details.

Immunofluorescence microscopy

For cell immunofluorescence staining, $1x10^5$ Mks at day 13 of culture were harvested and plated on collagen coated coverslips. Adhering cells were washed, fixed, permeabilzed and stained as previously described[29]. Please refer to Supplemental Methods for technical details.

Internalization assays

For immunofluorescence internalization assay, Mks were treated as living cells with 15 µg/mL of the anti-β1 integrin mAb (Abcam) and acid washed before fixation as previously described [31,32]. Mks were then fixed, permeabilized, and stained with the appropriate secondary antibody. Western blot internalization was evaluated as previously described [33]. Please refer to Supplemental Methods for technical details.

Silk film fabrication

Silk films were produced as previously described [34]. Type I or type IV collagen (25 µg/mL) were coated to the film surface overnight at 4°C. Please refer to Supplemental Methods for technical details.

Elastic modulus determination via Atomic Force Microscope (AFM)

Elastic modulus maps were taken on an Asylum Research MFP-3D AFM (Asylum Research) using AC240TS-R3 cantilevers (Asylum Research) with a nominal spring constant of 2 N/m. Please refer to Supplemental Methods for technical details.

$[Ca^{2+}]i$ measurements

Mks at day 13 of culture were harvested and plated onto substrate-coated cover-slips in 24-wells plates ($1x10^5$ cells/well). After 60 minutes at 37°C and 5% CO_2, Mks were loaded with 4 µM fura-2 AM in Physiological salt solution (PSS) for additional 30 minutes and analyzed as previously described[17]. Please refer to Supplemental Methods for technical details.

Animals and *in vivo* treatment

C57/BL6 wild type mice were from Charles River Laboratories. Mice were housed at the animal facility of the Department of Physiology, section of General Physiology, University of Pavia (approval # 1302/2015). All mice were sacrificed according to the current European legal Animal Practice requirements. *In vivo* Lysyl Oxidase (LOX) inhibition by BAPN treatment was carried out using a protocol modified from previous studies[35]. Please refer to Supplemental Methods for technical details.

In vivo bone marrow stiffness

The mechanical properties of femoral BM from mouse treated with BAPN and controls were measured with a Zwick/Roell Z005 testing device (Zwick GmbH & Co) equipped with a 10 N load cell as previously described[36]. Please refer to Supplemental Methods for technical details.

Flow cytometry

For the analysis of pAkt in BM Mks, femurs were flushed, red blood cells lysed with a 0.8% ammonium chloride solution, the remaining cells were washed by centrifugation with PBS and stained with anti-pAkt antibody (20 µL per test; BD Pharmingen) and anti-CD41 antibody (0.1 mg/mL; Biolegend) following the manufacturer instructions. All Mk samples, from the different tested sources, were routinely characterized as $CD41^{+}CD42b^{+}$ and $CD3^{-}CD4^{-}CD8^{-}CD11b^{-}CD19^{-}CD33^{-}$ cells, using appropriate antibodies (Beckman Coulter Inc.). Please refer to Supplemental Methods for technical details.

Bone marrow explant analysis

Bone marrow explants were isolated and analyzed based on a previous protocol [37]. Please refer to Supplemental Methods for technical details.

Statistics

Values are expressed as mean ± Standard Deviation (SD). *t test* was used to analyze experiments. A value of $p<0.05$ was considered statistically significant. All experiments were independently repeated at least three times.

For RT-PCR and quantitative real time PCR, tissue collection and immunohistochemistry, reticulated platelet analysis and LOX-mediated collagen crosslinking please refer to Supplemental Methods.

Results

Type I and type IV collagen differently impact megakaryocyte adhesion

To evaluate the impact of collagen stiffness on Mk behavior, coverslips were coated with type I or type IV collagens and Young's modulus was evaluated

by AFM-based nano-indentation[10,29]. As we previously demonstrated, type I collagen fibrils presented an elasticity >150 megapascal units (MPa), whereas material in early stage of self-aggregation had values in the order of 5-75 MPa[10]. On the contrary, more homogeneous values in the order of <10 MPa were found during the analysis of type IV collagen Young moduli. Consistently, nano-indentation studies on live cells plated on the two different collagens after 3 hours of adhesion revealed values ranging from 290 to 3,600 Pa (weighted average 1,036 Pa) in Mks plated on type I collagen, while values ranging from 300 to 1,400 Pa (weighted average 667 Pa) were obtained with Mks plated on type IV collagen (**Figure 1A**). As a result of the different stiffness, Mks remained spread over a 16 hours incubation on type I collagen, while they rearranged their cytoskeleton and extended proplatelets on type IV collagen (**Figure 1 B-C**).

Megakaryocyte β1 integrin activation and internalization vary depending on the type of collagen

We hypothesized that specific collagen receptors may be responsible of the observed Mk behavior on type I and type IV collagens. qRT-PCR analysis revealed that the most expressed collagen-interacting integrin domains were β1>α2, with DDR1 and GPVI expressed at a similar level as α2 (**Figure 2A**). As shown in **Figure 2A,** the most important reduction in Mk adhesion was obtained inhibiting β1 integrin, while DDR1 and GPVI inhibition did not significantly affect Mk adhesion relative to untreated controls[10,30]. β1 integrin activation was studied in Mks plated on type I and type IV collagens at the 3 time points used for functional studies (3, 8 and 16 hours), by employing a monoclonal antibody directed against epitopes in the 355–425 region (hybrid domain), whose expression reflects the activity of β1 integrin [38]. An increase of β1 integrin activation was observed on type IV collagen, compared to type I collagen, after 3 and 8 hours of adhesion, reaching a similar value under both conditions after 16 hours (**Figure 2B**). Consistently, internalization assays showed that membrane distributed β1 integrin was reduced on Mks plated on type IV collagen as compared to type I collagen (**Figure 2C**).

Substrate stiffness modulates β1 integrin dynamics

To prove that β1 integrin activation and internalization was determined by collagen substrate stiffness, silk fibroin films were fabricated with imposed elasticity and were afterwards coated with 25 μg/mL type I or type IV collagens[34]. Silk films with two different ranges of elasticity were chosen on the basis of previous results: a softer silk film (≤10 MPa) was chosen as the optimum condition to maximize Mk function, while a stiffer silk film (≥90 MPa) was chosen as a condition proven to decrease PPF[34]. Importantly, it is demonstrated that there are no specific cell-binding epitopes on the silk that would bias the outcomes[39]. As shown in **Figure 3A**, Mks extended proplatelets after 16 hours of adhesion on both collagens coated on soft films, while they maintained the spread form, independently on the collagen type, if plated on stiffer films. Lower stiffness promoted higher activation of the β1 integrin in Mks plated on both collagen type-coated silk films, as demonstrated by western blot and immunofluorescence staining (**Figure 3B, Supplemental Figure 1**), with increased β1 integrin internalization (**Figure 3C**).

PI3K/Akt-dependent proplatelet formation on soft collagen substrate

To understand the involvement of PI3K/Akt and MAPK/ERK signaling pathways in mediating the effect of soft collagen, Mks plated on type I and type IV collagen were lysed after 3, 8 and 16 hours. Western blot analysis demonstrated an important difference in Akt and ERK activation (**Figure 4A**). Specifically, ERK phosphorylation peaked after 3 hours on type I collagen, remaining higher up to 16 hours compared to type IV collagen, while Akt phosphorylation appeared constantly higher in Mks plated on type IV compared to type I collagen. Considering favorable PPF on type IV collagen, these results suggested a role for Akt phosphorylation as a positive mediator of PPF. Consistently, treatment of Mks plated on type IV collagen with a specific Akt inhibitor resulted in a significant reduction of PPF (**Figure 4A**). The role of substrate elasticity in Akt and ERK phosphorylation was further explored by using the silk fibroin film approach. Akt phosphorylation increased on soft collagen substrates, while ERK phosphorylation was unaffected (**Figure 4B**). Finally, inhibition of Akt in Mks plated on type I collagen-coated

soft films led to a reduction in PPF by about 80%, compared to untreated cells (**Figure 4B**). Accordingly, taking advantage of our system for platelet production through porous silk films [34], we showed that Akt inhibition significantly reduced the increase of platelet production obtained on soft collagen substrates (**Supplemental Figure 2**).

Megakaryocytes express functional mechano-sensitive TRPV4 ion channel

It has been demonstrated that, in endothelial cells, upon mechanical stress, β1 integrin activation determines the TRPV4 ion channel opening, which allows calcium influx inside the cell cytoplasm, supporting further β1 integrin engagement. Here, we show that human Mks expressed on their membrane functional TRPV4 ion channels (**Figure 5A-5B**) and that, upon adhesion onto type IV collagen, human Mks stained with FURA2-AM display calcium oscillations of significant higher frequency and amplitude than those observed during adhesion on type I collagen. Inhibition of TRPV4 channels with a selective antagonist (RN1734) led to a significant decrease in the amplitude of calcium spikes only on type IV collagen, but not on type I collagen, thus suggesting that calcium flux through TRPV4 differs in Mks plated on the two collagen types (**Figure 5C)**. The increased activation of TRPV4 on type IV collagen and on soft collagen substrates was also confirmed by immunoprecipitation of phosphorylated TRPV4 followed by western blot analysis (**Supplemental Figure 3**) [40].

β1 integrin activation, Akt phosphorylation and proplatelet formation on type IV collagen were sustained by TRPV4

To test whether TRPV4 channels mediate β1 integrin activation and Akt phosphorylation, both proteins were analyzed upon Mk treatment with a specific TRPV4 inhibitor (RN-1734) on type IV collagen and with a specific TRPV4 agonist (GSK1016790A) on type I collagen. Blocking TRPV4 activity with RN-1734 on type IV collagen resulted in a significant decrease of β1 integrin activation and Akt phosphorylation (**Figure 6A**). Consistently, the inhibition of TRPV4 activity resulted in diminished PPF on type IV collagen (**Figure 6B**), thus confirming the active role of the mechano-sensitive

TRPV4/β1integrin/Akt axis in PPF. On the contrary, forcing TRPV4 activation with GSK1016790A resulted in increased β1 integrin activation, Akt phosphorylation (**Figure 6C**) and β1 integrin internalization in Mks plated on type I collagen (**Figure 6D**).

Lysyl oxidase-mediated collagen crosslinking inhibition increases PPF and platelet production *in vivo*

A key regulator of collagen stiffness *in vivo* is the secreted enzyme lysyl oxidase (LOX), which by oxidative deamination of lysine residues on collagen, leads to cross-linked aldehydes, contributing to a tight and stiffer ECM [41]. To support the impact of collagen substrate elasticity on platelet production *in vivo*, mice were treated with a specific LOX inhibitor, which has been demonstrated to reduce tissue stiffness [42,43]. Inhibition of LOX, by beta-aminopropionitrile (BAPN) treatment, an irreversible inhibitor of LOX, diminished the bone marrow elastic modulus (**Figure 7A**) and reduced collagen fiber dimension in cortical bone (**Supplemental Figure 4**). As shown in **Figure 7B**, the reduction of bone marrow stiffness led to an increase in peripheral platelet count, while the count of the other blood cells was unchanged (**Supplemental Table 1**). The percentage of newly released reticulated platelets was significantly increased in treated mice, confirming that the boost in platelet numbers was mainly due to newly formed platelets (**Figure 7B**). Of note, the number of bone marrow Mks was not significantly affected by BAPN treatment, thus demonstrating that the increase in peripheral blood platelet counts was not due to a higher Mk number (**Supplemental Figure 5**). Interestingly, Akt phosphorylation was augmented in BAPN-treated bone marrow Mks as compared to CTRL by means of immunofluorescence imaging of bone marrow sections and flow cytometry analysis of flushed bone marrow (**Figure 7C**). To study PPF within bone marrow in LOX-inhibited and control mice, fresh bone marrow explants were examined by videomicroscopy (**Supplemental Figure 6**). Through this approach, Mks, recognized by their morphology, became visible at the periphery of the explant as round cells or as cells extending thick protrusions or proplatelets. Importantly, TRPV4 activation was analyzed in Mks explanted from these scenarios by evaluating the extent of TRPV4 phosphorylation,

which enhances TRPV4-mediated calcium inflow and may be employed as surrogate to monitor TRPV4 activation when the direct measurement of calcium signals is not feasible [40]. Diminishing the bone marrow stiffness resulted in an increase of TRPV4 activation in Mks as demonstrated by western blot analysis of immunoprecipitated TRPV4 (**Figure 8A**). Proplatelet forming Mks at 3 and 8 hours from the beginning of the experiment were quantified. The number of visible Mks per experiment was comparable in both conditions (CTRL 51±9 vs BAPN 58±13 at 3 hours; CTRL 63±14 vs BAPN 72±17 at 6 hours), while the percentage of proplatelet forming Mks was significantly higher in LOX-inhibited mice (**Figure 8B; Supplemental Video 1; Supplemental Video 2**). Importantly, Akt inhibition in bone marrow explants, from BAPN treated mice, reverted the increase in proplatelet formation to a level lower than CTRL mice (**Figure 8B; Supplemental Video 3**). Finally, to further explore the direct dependence of PPF on collagen substrate crosslinking and thus rigidity, PPF in Mks plated on type IV collagen pre-treated with recombinant LOXL2 protein was tested, in the presence or absence of BAPN. The incubation of type IV collagen with LOXL2 significantly reduced the percentage of proplatelet forming Mks, while inhibition of LOXL2 with BAPN rescued PPF to a level comparable to type IV collagen alone (**Supplemental Figure 7)**.

Discussion

The signaling pathways that control platelet formation in the bone marrow matrix environment have remained quite elusive. This study demonstrates that calcium influx through TRPV4 channels stimulates integrin β1 activation upon Mk adhesion on soft collagen substrate, promoting Akt phosphorylation and platelet formation. This previously unknown mechanism for platelet production adds new insights into the role of the ECM in regulating Mk function [44-46], and determines the importance of ECM-dependent calcium influx in regulating Mk spreading and PPF [17].

The bone marrow microenvironment consists of various ECM components that interact with each other to form a structural framework that supports

tissue organization and positional cues regulating megakaryopoiesis. In this structure, type I and IV are the most abundant collagens. Notably, type IV can support PPF [29], while type I collagen is the only ECM component known to inhibit this process [9,10,12]. This inhibition is triggered by the tensile strength of fibrils in type I collagen that regulates cytoskeleton contractility of Mks through activation of the Rho-ROCK pathway and MLC-2 phosphorylation [8,10]. Consistently, culturing Mks in a soft methylcellulose (MC) hydrogels, determines an increase of PPF through activation of the myosin IIA and MKL1 pathways [18].

The current data showed that type I collagen displayed a significant higher stiffness than type IV collagen, as revealed by AFM analysis. Consistently, only Mks plated on the softer type IV collagen extended long and branched proplatelets. We hypothesized that specific collagen receptors may regulate the different Mk behavior on type I and type IV collagens. Among the collagen receptors, integrins have been extensively described to be major mechano-receptors, due to their ability to modulate the signals transmitted inside the cell according to the physical properties of the ligand they bind [47]. In support of this hypothesis, the adhesion of Mks on both collagens was found to be mostly mediated by β1 integrin. However, β1 integrin was significantly more active and more internalized in Mks plated on type IV than on type I collagen during an 8 hours incubation time. These data were in line with the notion that β1 integrin dynamics and internalization-recycling circle are regulated by matrix stiffness [48,49]. Importantly, integrin detachment and internalization on soft substrate was previously shown in mesenchymal stromal cells, and was ascribed to the instability of the binding and, thus, to the low stress level necessary for the binding rupture [50]. In contrast, when the substrate stiffness increases, the relative number of nascent and retracting β1 integrin adhesions are reduced, and highly stable adhesions are promoted [51]. In accordance, by using passive silk films with different rigidities, substrate stiffness and β1 integrin activation in Mks were shown to be inversely proportional, as softer substrates promoted β1 integrin activation and internalization.

The increase in β1 integrin signaling that was observed on soft matrices, despite the higher rate of integrin internalization, is in line with recent work,

which demonstrated that endocytosis was necessary for full ECM-induced integrin mediated signaling [52]. PI3K/Akt and MAPK/ERK signaling pathways are known to be activated downstream β1 integrin and responsible for PPF regulation [13-17]. Interestingly, thrombocytopenia is one of the most frequent hematologic adverse events in patients treated with Perifosine, an oral Akt inhibitor used in cancer treatment [53]. Consistently, in our experiments, Akt and not ERK phosphorylation promoted Mk maturation and PPF upon β1 integrin activation by soft substrates. These data prompted us to hypothesize that other mechano-sensitive molecules may be involved in the regulation of these signaling processes. The mechano-sensitive ion channels, a member of which is TRPV4, seemed to be the best candidates to explain the data. First, these ion channels detect and transduce external mechanical forces into electrical and/or chemical intracellular signals [22,54]. Second, it was demonstrated that stretch-activated endothelial cells regulate Akt and ERK activation through a TRPV4-β1 integrin-dependent mechanism [24]. Consistently, in the experiments Mks were shown to express functional TRPV4 ion channels that were selectively activated only upon Mk adhesion on soft substrates.

Accordingly, TRPV4 channels present the unique ability to mediate an integrin-to-integrin signaling which is activated by mechanical forces transmitted by ECM components to β1 integrins. This results in the ultra-rapid (4 ms) alteration of the molecular conformation of TRPV4, which gates the channels and enables extracellular Ca2+ entry, thereby causing additional β1 activation [24,25,55].

Overall, these in vitro studies lead us to posit a model by which softer environment in the bone marrow promotes the activation of the TRPV4 ion channel that, in turns, leads to further β1 integrin stimulation and Akt phosphorylation, culminating with PPF. In line with this contention, adult mice treated with a specific LOX inhibitor that reduces tissue stiffness [42,43], promoted TRPV4, β1 integrin and Akt activation, with a consequent increase of platelet count in the peripheral blood. This occurred while Mk numbers in the bone marrow were not affected. Of note, an unexplained trend in increased platelet count was also reported earlier upon LOX inhibitor administration [35], although the dosage of inhibitor used in that study was low, and tested in newborn to young mice. A recent study showed that upregulated

LOX, at a level similar to that found in pathological bone marrow fibrosis, led to increased platelet adhesion to monomeric collagen mediated via α2β1 collagen receptors [56]. A similar increase in adhesion was observed with regard to LOX over-expressing Mks. Together with our current studies, we propose that LOX is capable of augmenting Mk adhesion via collagen receptor activation, but whether these Mks effectively produce proplatelets or not also depends on LOX-regulated ECM stiffness and changes in TRPV4 activation.

During life, ECM components are continuously rearranged to permit cell-tissue function. However, some patho-physiological conditions, such as aging or augmented bone marrow fibrosis determine an increase of ECM component rigidity, causing tissue function alterations [57,58]. Interestingly, it is known that platelet count is inversely correlated with age and that in the late stages of primary myelofibrosis, when the bone marrow is filled of thick reticular fibers, thrombocytopenia occurs [59,60]. Moreover, in these conditions, other organs, such as the lung [61] or the spleen [62], with a more favorable matrix environment, may become the site of platelet production. Based on these observations and on the mechanism described in the current work, we propose that beside the extensively described humoral-dependent mechanisms of platelet production, the physical properties of the ECM components that fill the bone marrow are crucial regulators of Mk function and platelet production.

Author contributions

Alessandra Balduini: supervised the project, conceived the idea, analyzed the data and wrote the manuscript. Vittorio Abbonante: conceived the idea, designed and performed the experiments, analyzed the data and wrote the manuscript. Christian A. Di Buduo, Cristian Gruppi, Carmelo De Maria, Elise Spedden, Aurora De Acutis and Mario Raspanti: performed the experiments and edited the manuscript; Cristian Staii, Giovanni Vozzi, David L. Kaplan, Francesco Moccia and Katya Ravid: analyzed the data and edited the manuscript.

Conflict of interests

The authors declare no conflict of interests.

References

1. Machlus KR, Italiano JE. The incredible journey: From megakaryocyte development to platelet formation. J Cell Biol. 2013;201(6):785-796.
2. Patel SR, Richardson JL, Schulze H, et al. Differential roles of microtubule assembly and sliding in proplatelet formation by megakaryocytes. Blood. 2005;106(13):4076-4085.
3. Junt T, Schulze H, Chen Z, et al. Dynamic visualization of thrombopoiesis within bone marrow. Science. 2007;317(5845):1767-1770.
4. Malara A, Abbonante V, Di Buduo CA, Tozzi L, Currao M, Balduini A. The secret life of a megakaryocyte: emerging roles in bone marrow homeostasis control. Cell Mol Life Sci. 2015;72(8):1517-1536.
5. Hynes RO. The extracellular matrix: not just pretty fibrils. Science. 2009;326(5957):1216-1219.
6. Gattazzo F, Urciuolo A, Bonaldo P. Extracellular matrix: a dynamic microenvironment for stem cell niche. Biochim Biophys Acta. 2014;1840(8):2506-2519.
7. Mouw JK, Ou G, Weaver VM. Extracellular matrix assembly: a multiscale deconstruction. Nat Rev Mol Cell Biol. 2014;15(12):771-785.
8. Shin JW, Swift J, Spinler KR, Discher DE. Myosin-II inhibition and soft 2D matrix maximize multinucleation and cellular projections typical of platelet-producing megakaryocytes. Proc Natl Acad Sci U S A. 2011;108(28):11458-11463.
9. Chen Z, Naveiras O, Balduini A, et al. The May-Hegglin anomaly gene MYH9 is a negative regulator of platelet biogenesis modulated by the Rho-ROCK pathway. Blood. 2007;110(1):171-179.
10. Malara A, Gruppi C, Pallotta I, et al. Extracellular matrix structure and nano-mechanics determine megakaryocyte function. Blood. 2011;118(16):4449-4453.
11. Chang Y, Auradé F, Larbret F, et al. Proplatelet formation is regulated by the Rho/ROCK pathway. Blood. 2007;109(10):4229-4236.
12. Semeniak D, Kulawig R, Stegner D, et al. Proplatelet formation is selectively inhibited by collagen type I through Syk-independent GPVI signaling. J Cell Sci. 2016;129(18):3473-3484.
13. Machlus KR, Johnson KE, Kulenthirarajan R, et al. CCL5 derived from platelets increases megakaryocyte proplatelet formation. Blood. 2016;127(7):921-926.
14. Bluteau D, Balduini A, Balayn N, et al. Thrombocytopenia-associated mutations in the ANKRD26 regulatory region induce MAPK hyperactivation. J Clin Invest. 2014;124(2):580-591.
15. Mazharian A, Watson SP, Séverin S. Critical role for ERK1/2 in bone marrow and fetal liver-derived primary megakaryocyte differentiation, motility, and proplatelet formation. Exp Hematol. 2009;37(10):1238-1249.e1235.
16. Currao M, Balduini CL, Balduini A. High doses of romiplostim induce proliferation and reduce proplatelet formation by human megakaryocytes. PLoS One. 2013;8(1):e54723.
17. Di Buduo CA, Moccia F, Battiston M, et al. The importance of calcium in the regulation of megakaryocyte function. Haematologica. 2014;99(4):769-778.

18. Aguilar A, Pertuy F, Eckly A, et al. Importance of environmental stiffness for megakaryocyte differentiation and proplatelet formation. Blood. 2016.
19. Giancotti FG, Ruoslahti E. Integrin signaling. Science. 1999;285(5430):1028-1032.
20. Campbell ID, Humphries MJ. Integrin structure, activation, and interactions. Cold Spring Harb Perspect Biol. 2011;3(3).
21. Schwartz MA. Integrins and extracellular matrix in mechanotransduction. Cold Spring Harb Perspect Biol. 2010;2(12):a005066.
22. Gasparski AN, Beningo KA. Mechanoreception at the cell membrane: More than the integrins. Arch Biochem Biophys. 2015;586:20-26.
23. Martinac B. Mechanosensitive ion channels: an evolutionary and scientific tour de force in mechanobiology. Channels (Austin). 2012;6(4):211-213.
24. Thodeti CK, Matthews B, Ravi A, et al. TRPV4 channels mediate cyclic strain-induced endothelial cell reorientation through integrin-to-integrin signaling. Circ Res. 2009;104(9):1123-1130.
25. Matthews BD, Thodeti CK, Tytell JD, Mammoto A, Overby DR, Ingber DE. Ultra-rapid activation of TRPV4 ion channels by mechanical forces applied to cell surface beta1 integrins. Integr Biol (Camb). 2010;2(9):435-442.
26. Jablonski CL, Ferguson S, Pozzi A, Clark AL. Integrin α1β1 participates in chondrocyte transduction of osmotic stress. Biochem Biophys Res Commun. 2014;445(1):184-190.
27. Kröger N, Zabelina T, Alchalby H, et al. Dynamic of bone marrow fibrosis regression predicts survival after allogeneic stem cell transplantation for myelofibrosis. Biol Blood Marrow Transplant. 2014;20(6):812-815.
28. Abbonante V, Di Buduo CA, Gruppi C, et al. Thrombopoietin/TGF-β1 loop regulates megakaryocyte extracellular matrix component synthesis. Stem Cells. 2016.
29. Balduini A, Pallotta I, Malara A, et al. Adhesive receptors, extracellular proteins and myosin IIA orchestrate proplatelet formation by human megakaryocytes. J Thromb Haemost. 2008;6(11):1900-1907.
30. Abbonante V, Gruppi C, Rubel D, Gross O, Moratti R, Balduini A. Discoidin domain receptor 1 protein is a novel modulator of megakaryocyte-collagen interactions. J Biol Chem. 2013;288(23):16738-16746.
31. Lampugnani MG, Orsenigo F, Gagliani MC, Tacchetti C, Dejana E. Vascular endothelial cadherin controls VEGFR-2 internalization and signaling from intracellular compartments. J Cell Biol. 2006;174(4):593-604.
32. Lawson MA, Maxfield FR. Ca(2+)- and calcineurin-dependent recycling of an integrin to the front of migrating neutrophils. Nature. 1995;377(6544):75-79.
33. Fabbri M, Di Meglio S, Gagliani MC, et al. Dynamic partitioning into lipid rafts controls the endo-exocytic cycle of the alphaL/beta2 integrin, LFA-1, during leukocyte chemotaxis. Mol Biol Cell. 2005;16(12):5793-5803.
34. Di Buduo CA, Wray LS, Tozzi L, et al. Programmable 3D silk bone marrow niche for platelet generation ex vivo and modeling of megakaryopoiesis pathologies. Blood. 2015;125(14):2254-2264.
35. Eliades A, Papadantonakis N, Bhupatiraju A, et al. Control of megakaryocyte expansion and bone marrow fibrosis by lysyl oxidase. J Biol Chem. 2011;286(31):27630-27638.
36. Urciuolo A, Quarta M, Morbidoni V, et al. Collagen VI regulates satellite cell self-renewal and muscle regeneration. Nat Commun. 2013;4:1964.

37. Eckly A, Rinckel JY, Laeuffer P, et al. Proplatelet formation deficit and megakaryocyte death contribute to thrombocytopenia in Myh9 knockout mice. J Thromb Haemost. 2010;8(10):2243-2251.
38. Luque A, Gómez M, Puzon W, Takada Y, Sánchez-Madrid F, Cabañas C. Activated conformations of very late activation integrins detected by a group of antibodies (HUTS) specific for a novel regulatory region (355-425) of the common beta 1 chain. J Biol Chem. 1996;271(19):11067-11075.
39. Zhou CZ, Confalonieri F, Jacquet M, Perasso R, Li ZG, Janin J. Silk fibroin: structural implications of a remarkable amino acid sequence. Proteins. 2001;44(2):119-122.
40. Fan HC, Zhang X, McNaughton PA. Activation of the TRPV4 ion channel is enhanced by phosphorylation. J Biol Chem. 2009;284(41):27884-27891.
41. Papadantonakis N, Matsuura S, Ravid K. Megakaryocyte pathology and bone marrow fibrosis: the lysyl oxidase connection. Blood. 2012;120(9):1774-1781.
42. Marturano JE, Xylas JF, Sridharan GV, Georgakoudi I, Kuo CK. Lysyl oxidase-mediated collagen crosslinks may be assessed as markers of functional properties of tendon tissue formation. Acta Biomater. 2014;10(3):1370-1379.
43. Mammoto A, Mammoto T, Kanapathipillai M, et al. Control of lung vascular permeability and endotoxin-induced pulmonary oedema by changes in extracellular matrix mechanics. Nat Commun. 2013;4:1759.
44. Malara A, Currao M, Gruppi C, et al. Megakaryocytes contribute to the bone marrow-matrix environment by expressing fibronectin, type IV collagen, and laminin. Stem Cells. 2014;32(4):926-937.
45. Ivanovska IL, Shin JW, Swift J, Discher DE. Stem cell mechanobiology: diverse lessons from bone marrow. Trends Cell Biol. 2015;25(9):523-532.
46. Choi JS, Harley BA. The combined influence of substrate elasticity and ligand density on the viability and biophysical properties of hematopoietic stem and progenitor cells. Biomaterials. 2012;33(18):4460-4468.
47. Schwarz US, Gardel ML. United we stand: integrating the actin cytoskeleton and cell-matrix adhesions in cellular mechanotransduction. J Cell Sci. 2012;125(Pt 13):3051-3060.
48. Pellinen T, Ivaska J. Integrin traffic. J Cell Sci. 2006;119(Pt 18):3723-3731.
49. Bridgewater RE, Norman JC, Caswell PT. Integrin trafficking at a glance. J Cell Sci. 2012;125(Pt 16):3695-3701.
50. Du J, Chen X, Liang X, et al. Integrin activation and internalization on soft ECM as a mechanism of induction of stem cell differentiation by ECM elasticity. Proc Natl Acad Sci U S A. 2011;108(23):9466-9471.
51. Doyle AD, Carvajal N, Jin A, Matsumoto K, Yamada KM. Local 3D matrix microenvironment regulates cell migration through spatiotemporal dynamics of contractility-dependent adhesions. Nat Commun. 2015;6:8720.
52. Alanko J, Mai A, Jacquemet G, et al. Integrin endosomal signalling suppresses anoikis. Nat Cell Biol. 2015;17(11):1412-1421.
53. Richardson PG, Eng C, Kolesar J, Hideshima T, Anderson KC. Perifosine , an oral, anti-cancer agent and inhibitor of the Akt pathway: mechanistic actions, pharmacodynamics, pharmacokinetics, and clinical activity. Expert Opin Drug Metab Toxicol. 2012;8(5):623-633.
54. Garcia-Elias A, Mrkonjić S, Jung C, Pardo-Pastor C, Vicente R, Valverde MA. The TRPV4 channel. Handb Exp Pharmacol. 2014;222:293-319.

55. White JP, Cibelli M, Urban L, Nilius B, McGeown JG, Nagy I. TRPV4: Molecular Conductor of a Diverse Orchestra. Physiol Rev. 2016;96(3):911-973.
56. Matsuura S, Mi R, Koupenova M, et al. Lysyl oxidase is associated with increased thrombosis and platelet reactivity. Blood. 2016;127(11):1493-1501.
57. Lu P, Weaver VM, Werb Z. The extracellular matrix: a dynamic niche in cancer progression. J Cell Biol. 2012;196(4):395-406.
58. Kurtz A, Oh SJ. Age related changes of the extracellular matrix and stem cell maintenance. Prev Med. 2012;54 Suppl:S50-56.
59. Balduini CL, Noris P. Platelet count and aging. Haematologica. 2014;99(6):953-955.
60. Cervantes F, Barosi G. Myelofibrosis with myeloid metaplasia: diagnosis, prognostic factors, and staging. Semin Oncol. 2005;32(4):395-402.
61. Wang Y, Hayes V, Jarocha D, et al. Comparative analysis of human ex vivo-generated platelets vs megakaryocyte-generated platelets in mice: a cautionary tale. Blood. 2015;125(23):3627-3636.
62. Thiele J, Klein H, Falk S, Bertsch HP, Fischer R, Stutte HJ. Splenic megakaryocytopoiesis in primary (idiopathic) osteomyelofibrosis. An immunohistological and morphometric study with comparison of corresponding bone marrow features. Acta Haematol. 1992;87(4):176-180.

Figure legends

Figure 1. Type I and type IV collagens differently regulate megakaryocyte adhesion. A) Distribution of Young's modulus values of live Mks plated on type I and type IV collagens. Three independent experiments were performed. B) Human mature Mks, 1 x 10^5 per well in 24 well plates, were plated on type I and type IV collagen coated coverslips for three different time. Cells were fixed and stained with anti-β1 tubulin (green) and tetramethylrhodamine (TRITC)-Phalloidin (red). Nuclei were counterstained with Hoechst (blue). Scale bar 50 μm; box scale bar 20 μm. C) Mks exhibiting stress fibers were counted and presented as percentage of spread Mk, while Mks extending proplatelets were counted and shown as percentage of proplatelet bearing Mks. Results shown in panels C are mean ± SD of six independent experiments; * $p<0.05$.

Figure 2. β1 integrin is strongly involved in mediating megakaryocyte adhesion on type I and type IV collagens. A) Analysis of collagen receptors. qRT-PCR analysis of different collagen receptors in human mature Mks (left panel). Data are shown as mean ± SD, of four independent experiments, relative to the housekeeping gene β2-microglobulin. Mk adhesion on type I and IV collagens was evaluated upon treatment with different collagen receptor blocking antibodies or blocking molecules (10 μg/mL anti-β1 integrin, 200 nM DDR1-IN-1, 10 μg/mL anti-GPVI) (right panel). Data are shown as mean percentage of adhering Mks ± SD, of five independent experiments, relative to untreated cells. B) Western blot analysis of active β1 integrin in Mks plated on type I and type IV collagens for different times. Total β1 integrin and actin were determined to show equal loading. The densitometry analysis of active β1 integrin level, derived from three independent experiments, is shown. C) β1 integrin internalization assays. Western blot analysis of internalized β1 integrin after 1, 3 and 8 hours of adhesion on type I and type IV collagens (upper panel). To show equal loading actin was determined on total cell lysates. The first lane on the left represents the positive control of untreated Mks. The densitometry analysis of

internalized β1 integrin level, derived from four independent experiments, is shown. Immunofluorescence analysis of internalized β1 integrin in Mks plated on type I and type IV collagens for 3 hours (bottom panel). Mks were stained with anti-β1 integrin (green) and TRITC-Phalloidin (red). Nuclei were counterstained with Hoechst (blue). Scale bar 10 µm. The densitometry analysis of staining intensities, derived from four independent experiments, is shown. A minimum of 20 cells per experiment was evaluated. Data of densitometry analysis are all expressed as mean ± SD; * $p<0.05$.

Figure 3. Collagen substrate elasticity regulates β1 integrin dynamics and proplatelet formation. A) Mks extending proplatelets were counted and shown as percentage of proplatelet bearing Mks. Data are expressed as mean percentage ± SD of eight independent experiments. B) Western blot analysis of active β1 integrin in Mks plated on type I and type IV collagen coated soft and stiff silk fibroin films. Total β1 integrin and actin were determined to show equal protein loading. The densitometry analysis of active β1 integrin level, derived form four independent experiments is shown. C) β1 integrin internalization assays. Western blot analysis of internalized β1 integrin after 1, 3 and 8 hours of adhesion on type I collagen-coated soft and stiff silk fibroin films (left panel). Actin, in total cell lysates, was determined to show equal loading. The first lane on the left represents the positive control of untreated Mks. The densitometry analysis of internalized β1 integrin level, derived form four independent experiments, is shown. Immunofluorescence analysis of internalized β1 integrin in Mks plated on type I collagen-coated soft and stiff silk fibroin films for 3 hours (right panel). Cells were stained with anti-β1 integrin (green) and TRITC-Phalloidin (red). Nuclei were counterstained with Hoechst (blue). Scale bar 10 µm. The densitometry analysis of staining intensities, derived form four independent experiments, is shown. A minimum of 20 cells per experiment was evaluated. Data of densitometry analysis are all expressed as mean ± SD; * $p<0.05$ **$p<0.01$.

Figure 4. PI3K/Akt signaling mediates proplatelet formation on soft collagen substrates. A) Western blot analysis of Akt and ERK phosphorylation (pAkt and pERK) in Mks plated for 3, 8 and 16 hours on type

I and type IV collagens (left panel). Total Akt, ERK and actin were determined to show the equal loading. The densitometry analysis of pAkt and pERK level, derived from four independent experiments, is shown. Proplatelet formation assay in Mks plated for 16 hours on type IV collagen in presence or not of 10 μM Akt inhibitor (right panel). Mks extending proplatelet were counted and shown as percentage of proplatelet bearing Mks. Data are expressed as mean percentage ± SD of five independent experiments. B) Western blot analysis of pAkt and pERK in Mks plated for 3 hours on type I and type IV collagen coated soft and stiff silk fibroin films (left panel). Total Akt, ERK and actin were determined to show equal loading. The densitometry analysis of pAkt and pERK level, derived from five independent experiments, is shown. Proplatelet formation assay in Mks plated for 16 hours on type I collagen coated soft silk fibroin films in presence or not of 10 μM Akt inhibitor (right panel). Mks extending proplatelets were counted and expressed as percentage of proplatelet bearing MKs. Data are expressed as mean percentage ± SD of five independent experiments. Data of densitometry analysis are all expressed as mean ± SD; * $p<0.05$.

Figure 5. Megakaryocytes express a functional TRPV4 ion channel. A) TRPV4 expression in mature Mks. RT-PCR analysis of TRPV4 (left panel). Western blot analysis of TRPV4 (right panel). B) Functional characterization of TRPV4. Analysis of calcium signaling in response to 10 nM GSK1016790A (TRPV4 agonist) in FURA2–AM loaded Mks pretreated or not, for 60 minutes, with 10 μM of the indicated TRPV4 inhibitor (RN-1734 or HC067047) (left panel). GSK1016790A was added at 100 seconds from the beginning of the analysis. Data are representative of three independent experiments. A minimum of 40 Mks per experiment was evaluated. In absence of extracellular calcium ($0Ca^{2+}$) treatment with 10 nM GSK1016790A did not elicited significant changes in calcium signaling in FURA2–AM loaded Mks (right panel). After extracellular calcium restoration, in presence of GSK1016790A, the increase in Mks fluorescence was indicative of extracellular calcium entry in Mks cytosol. GSK1016790A was added after 300 seconds from the beginning of the experiment. Data are representative of three independent experiments. A minimum of 40 Mks per experiment was evaluated. C) TRPV4

activity on type I and IV collagens. Number of calcium peaks per Mks plated on type I and type IV collagens in presence or not of 10 μM RN-1734. Time of analysis was 800 seconds. Calcium peak amplitude in megakaryocytes plated on type I and type IV collagens in presence or not of 10 μM RN-1734 (left panel). Representative calcium oscillations in Mks plated on type I and type IV collagens (right panel). RN-1734 was added at 600 seconds from the beginning of the analysis. Data in panels C refers to eight independent experiments. Data are expressed as mean ± SD; * $p< 0.05$ ** $p<0.01$.

Figure 6. TRPV4 activity regulates β1 integrin dynamics and Akt phosphorylation. A) Western blot analysis of active β1 integrin and phosphorylated Akt (pAkt) in Mks plated on type IV collagen in presence or not of 10 μM RN-1734 (RN). Total β1 integrin, Akt and actin were determined to show equal loading. The densitometry analysis of active β1 integrin level and pAkt, derived form four independent experiments is shown. B) Proplatelet formation assay in Mks plated on type IV collagen in presence or not of 10 μM RN-1734. Proplatelet bearing Mks were counted and shown as percentages of proplatelet bearing Mks. Data are shown as mean percentage ± SD of six independent experiments. C) Western blot analysis of active β1 integrin and pAkt in Mks plated on type I collagen in presence or not of 10 nM GSK1016790A (GSK). Total β1 integrin, Akt and actin were determined to show equal loading. The densitometry analysis of active β1 integrin level and pAkt, derived form four independent experiments, is shown. β1 integrin internalization assays. D) Immunofluorescence analysis of internalized β1 integrin in Mks plated on type I collagen in presence or not of 10 nM GSK1016790A (left panel). Cells were stained with anti-β1 integrin (green) and TRITC-Phalloidin (red). Nuclei were counterstained with Hoechst (blue). Scale bar 5 μm. The densitometry analysis of staining intensities, derived form three independent experiments, is shown. A minimum of 20 cells per experiments was evaluated. Western blot analysis of internalized β1 integrin in megakaryocytes plated on type I collagen in presence or not of 10 nM GSK1016790A (right panel). To show equal loading actin was determined on total cell lysates. The densitometry analysis of internalized β1 integrin level,

derived form three independent experiments is shown. Data of densitometry analysis are all expressed as mean ± SD; * $p<0.05$.

Figure 7. Lysyl oxidase-mediated collagen crosslinking inhibition increases platelet production *in vivo*. A) Elastic modulus of untreated (CTRL) and BAPN-treated mice bone marrows. Data refers to four different mice per group. Bone marrow from both femurs per mouse was analyzed. B) Peripheral blood platelet count of untreated (CTRL) and BAPN-treated mice. Data refers to ten mice per group. Reticulated platelet measurements in peripheral blood of untreated (CTRL) and BAPN-treated mice. Data refers to eight mice per group. C) pAkt analysis in CTRL and BAPN treated mouse Mks was performed by BM section immunofluorescence (left panel) and by flow cytometry (right panel). The densitometry analysis of pAkt immunofluorescence staining, of bone marrow Mks, is derived from four mice per group. At least 30 Mks per section were analyzed. The flow cytometry analysis of pAkt phosphorylation was performed in CD41+ bone marrow Mks. The mean fluorescence intensity (MFI) is shown. Data are expressed as mean ± SD of five independent experiments. Data of densitometry analysis are all expressed as mean ± SD; * $p<0.05$.

Figure 8. Lysyl oxidase-mediated collagen crosslinking inhibition increases proplatelet formation and TRPV4 activation *ex vivo*. A) Western blot analysis of TRPV4 immunoprecipitated from bone marrow immunomagnetically-sorted Mks. A control sample was immunoprecipitated with an unrelated antibody (IgG). Membranes were probed with anti-PKC-substrates antibody (recognizing phosphorylated serine) and with anti-TRPV4 antibody. Actin staining on total cell lysates is shown to ensure equal loading. The densitometry analysis of the phosphorylated TRPV4/total TRPV4 ratio is shown. Data refers to three independent experiments. B) Proplatelet formation assay in BM explants. Mks extending proplatelet were counted after 3 and 8 hours from the beginning of the experiment, and shown is the percentage of proplatelet bearing Mks. Data are expressed as mean percentage ± SD. n = 10 CTRL, 10 BAPN, 3 BAPN + AKT inhibitor (AKT INH). C) Representative pictures of proplatelet bearing Mks in bone marrow

explants. Mks were stained as living cells with anti-CD41-FITC antibody. Data of densitometry analysis are expressed as mean ± SD; Scale bar = 50 μm upper pictures; 100 μm lower pictures. * $p<0.05$.

FIGURE 1

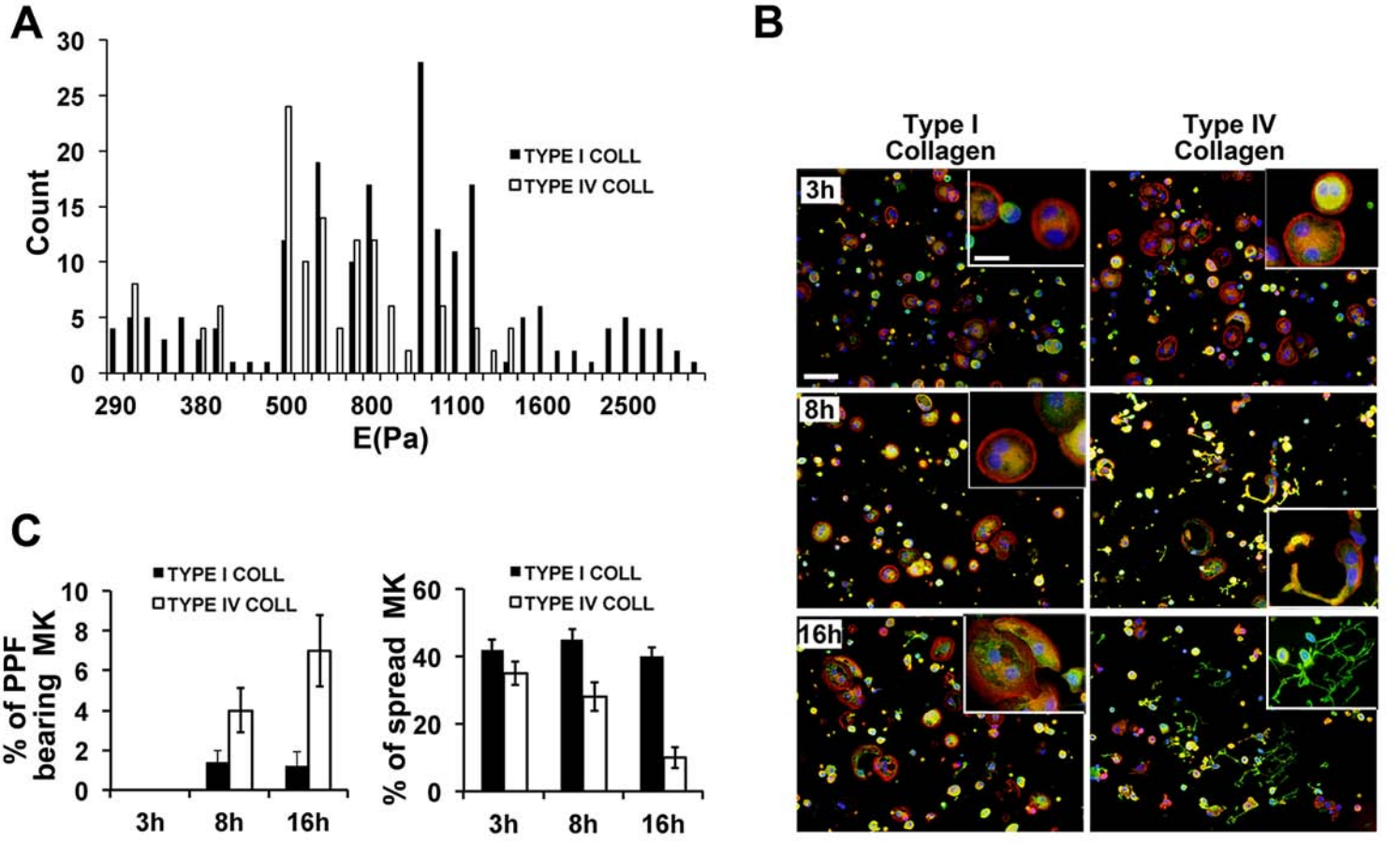
A
Count
E(Pa)
TYPE I COLL
TYPE IV COLL
B
Type I Collagen
Type IV Collagen
3h
8h
16h
C
% of PPF bearing MK
% of spread MK
TYPE I COLL
TYPE IV COLL
3h
8h
16h

FIGURE 2

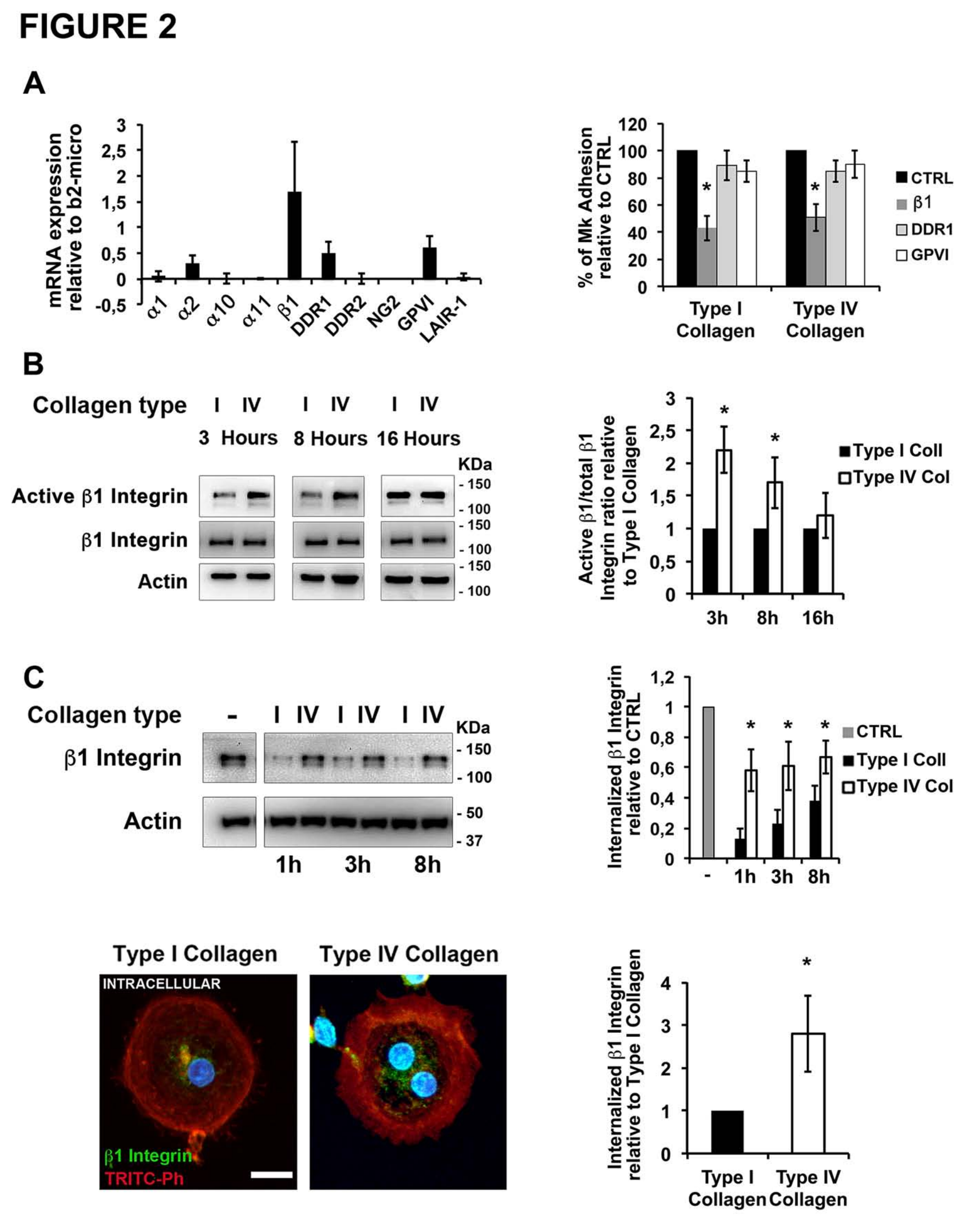
A
mRNA expression relative to b2-micro
3
2,5
2
1,5
1
0,5
0
-0,5
α1
α2
α10
α11
β1
DDR1
DDR2
NG2
GPVI
LAIR-1
% of Mk Adhesion relative to CTRL
120
100
80
60
40
20
0
*
*
CTRL
β1
DDR1
GPVI
Type I Collagen
Type IV Collagen
B
Collagen type I IV I IV I IV
3 Hours
8 Hours
16 Hours
KDa
Active β1 Integrin
β1 Integrin
Actin
- 150
- 100
- 150
- 100
- 150
- 100
Active β1/total β1 Integrin ratio relative to Type I Collagen
3
2,5
2
1,5
1
0,5
0
*
*
Type I Coll
Type IV Col
3h
8h
16h
C
Collagen type - I IV I IV I IV
KDa
β1 Integrin
Actin
- 150
- 100
- 50
- 37
1h
3h
8h
Internalized β1 Integrin relative to CTRL
1,2
1
0,8
0,6
0,4
0,2
0
*
*
*
CTRL
Type I Coll
Type IV Col
-
1h
3h
8h
Type I Collagen
Type IV Collagen
INTRACELLULAR
β1 Integrin
TRITC-Ph
Internalized β1 Integrin relative to Type I Collagen
4
3
2
1
0
*
Type I Collagen
Type IV Collagen

FIGURE 3

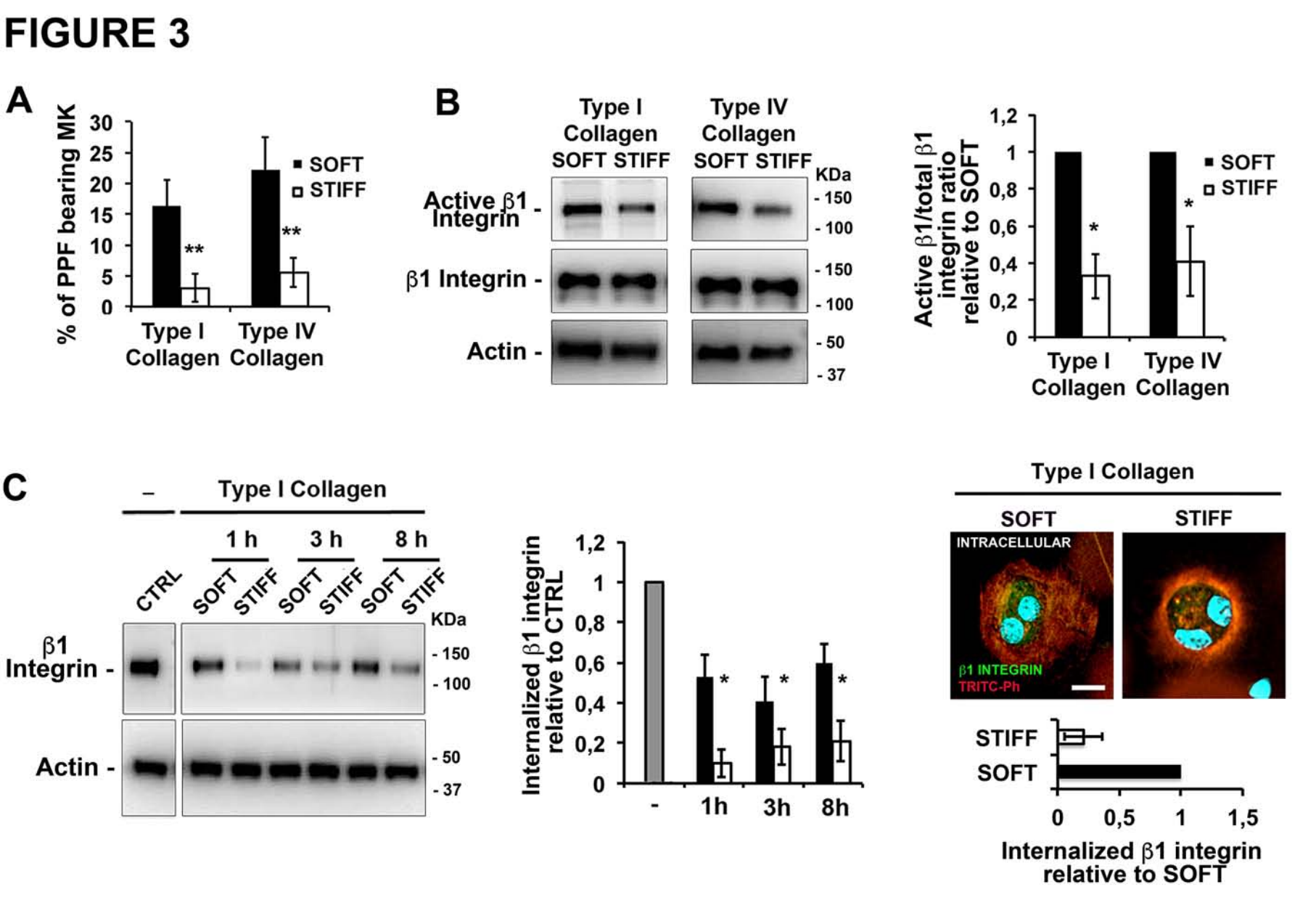
A
% of PPF bearing MK
30
25
20
15
10
5
0
SOFT
STIFF
**
**
Type I Collagen
Type IV Collagen
B
Type I Collagen
Type IV Collagen
SOFT STIFF
SOFT STIFF
KDa
Active β1 Integrin -
β1 Integrin -
Actin -
- 150
- 100
- 150
- 100
- 50
- 37
Active β1/total β1 integrin ratio relative to SOFT
1,2
1
0,8
0,6
0,4
0,2
0
SOFT
STIFF
*
*
Type I Collagen
Type IV Collagen
C
–
Type I Collagen
1 h
3 h
8 h
CTRL
SOFT
STIFF
SOFT
STIFF
SOFT
STIFF
KDa
β1 Integrin -
Actin -
- 150
- 100
- 50
- 37
Internalized β1 integrin relative to CTRL
1,2
1
0,8
0,6
0,4
0,2
0
*
*
*
-
1h
3h
8h
Type I Collagen
SOFT
STIFF
INTRACELLULAR
β1 INTEGRIN
TRITC-Ph
STIFF
SOFT
0
0,5
1
1,5
Internalized β1 integrin relative to SOFT

FIGURE 4

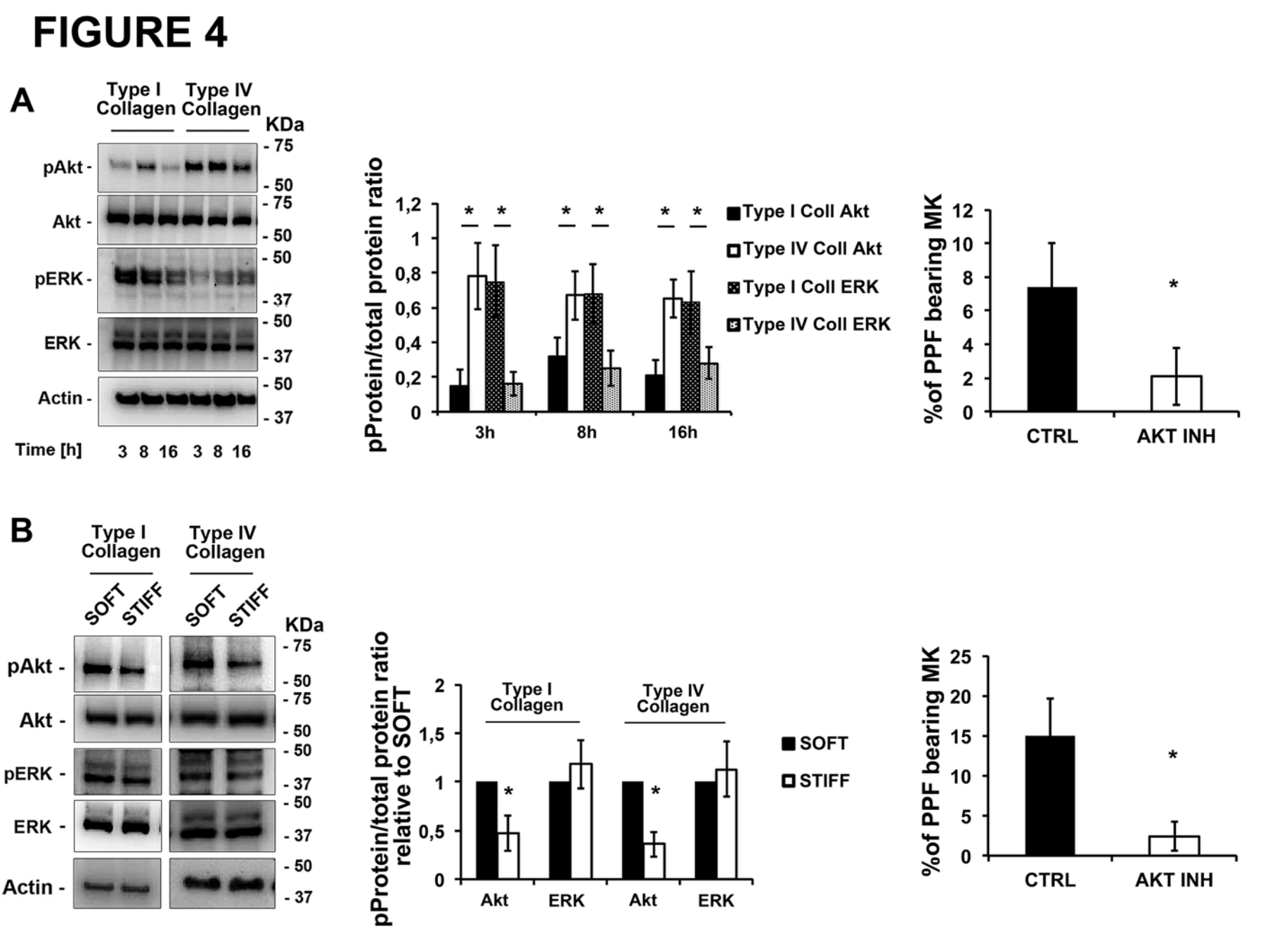
A
Type I Collagen
Type IV Collagen
KDa
pAkt
Akt
pERK
ERK
Actin
- 75
- 50
- 37
Time [h]
3 8 16 3 8 16
pProtein/total protein ratio
1,2
1
0,8
0,6
0,4
0,2
0
3h
8h
16h
Type I Coll Akt
Type IV Coll Akt
Type I Coll ERK
Type IV Coll ERK
%of PPF bearing MK
12
10
8
6
4
2
0
CTRL
AKT INH
B
Type I Collagen
Type IV Collagen
SOFT
STIFF
KDa
pAkt
Akt
pERK
ERK
Actin
- 75
- 50
- 37
pProtein/total protein ratio relative to SOFT
2
1,5
1
0,5
0
Akt
ERK
SOFT
STIFF
%of PPF bearing MK
25
20
15
10
5
0
CTRL
AKT INH

FIGURE 5

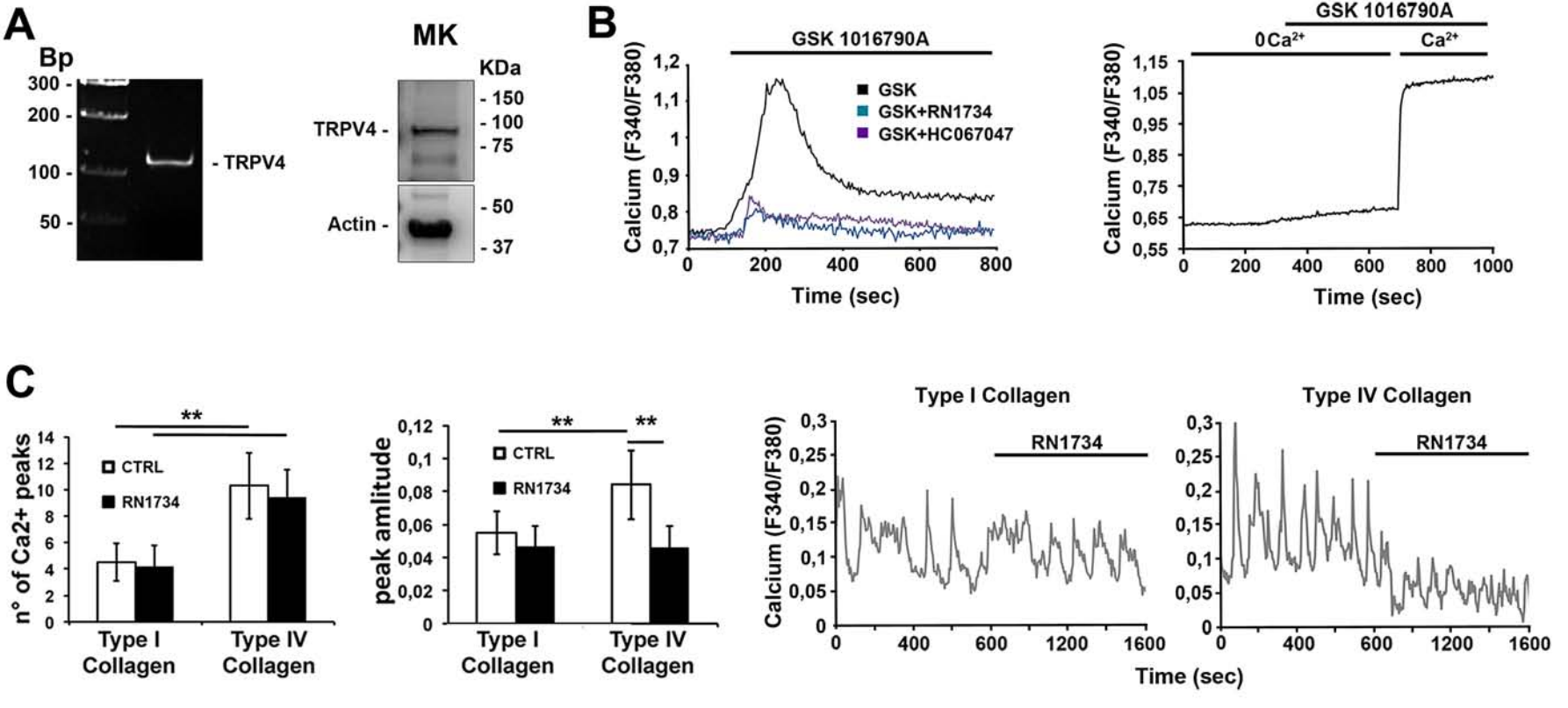
A
Bp
300 -
200 -
100 -
50 -
- TRPV4
MK
KDa
TRPV4 -
Actin -
- 150
- 100
- 75
- 50
- 37
B
GSK 1016790A
GSK
GSK+RN1734
GSK+HC067047
Calcium (F340/F380)
Time (sec)
GSK 1016790A
0Ca2+
Ca2+
C
n° of Ca2+ peaks
CTRL
RN1734
Type I Collagen
Type IV Collagen
peak amlitude
Type I Collagen
RN1734
Type IV Collagen
RN1734
Calcium (F340/F380)
Time (sec)

FIGURE 6

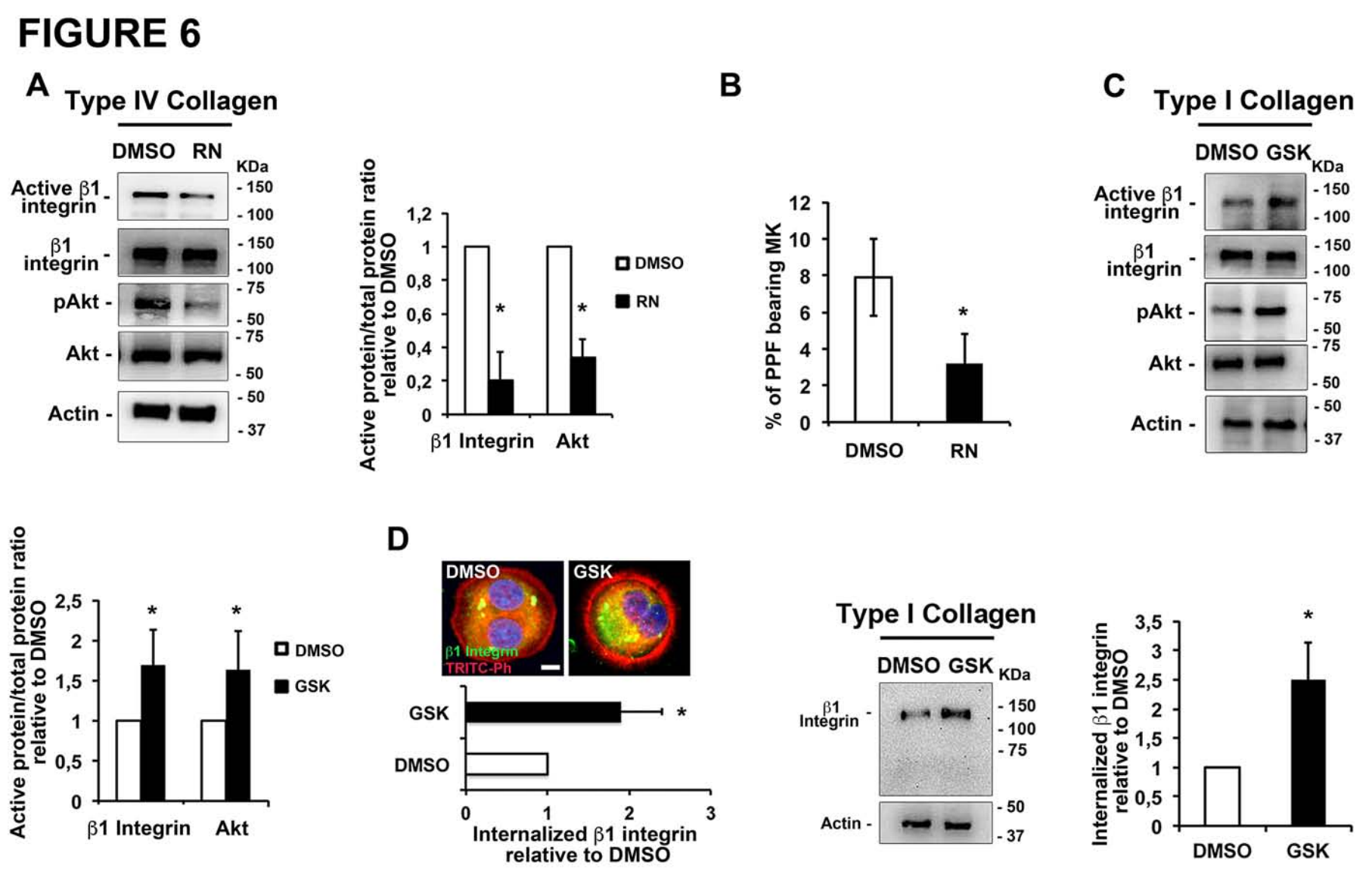
A
Type IV Collagen
DMSO RN
KDa
Active β1 integrin
β1 integrin
pAkt
Akt
Actin
150
100
75
50
37
Active protein/total protein ratio relative to DMSO
DMSO
RN
β1 Integrin
Akt
B
% of PPF bearing MK
DMSO
RN
C
Type I Collagen
DMSO GSK
D
DMSO
GSK
β1 integrin
TRITC-Ph
Internalized β1 integrin relative to DMSO
Type I Collagen
β1 Integrin
Actin
Internalized β1 integrin relative to DMSO

FIGURE 7

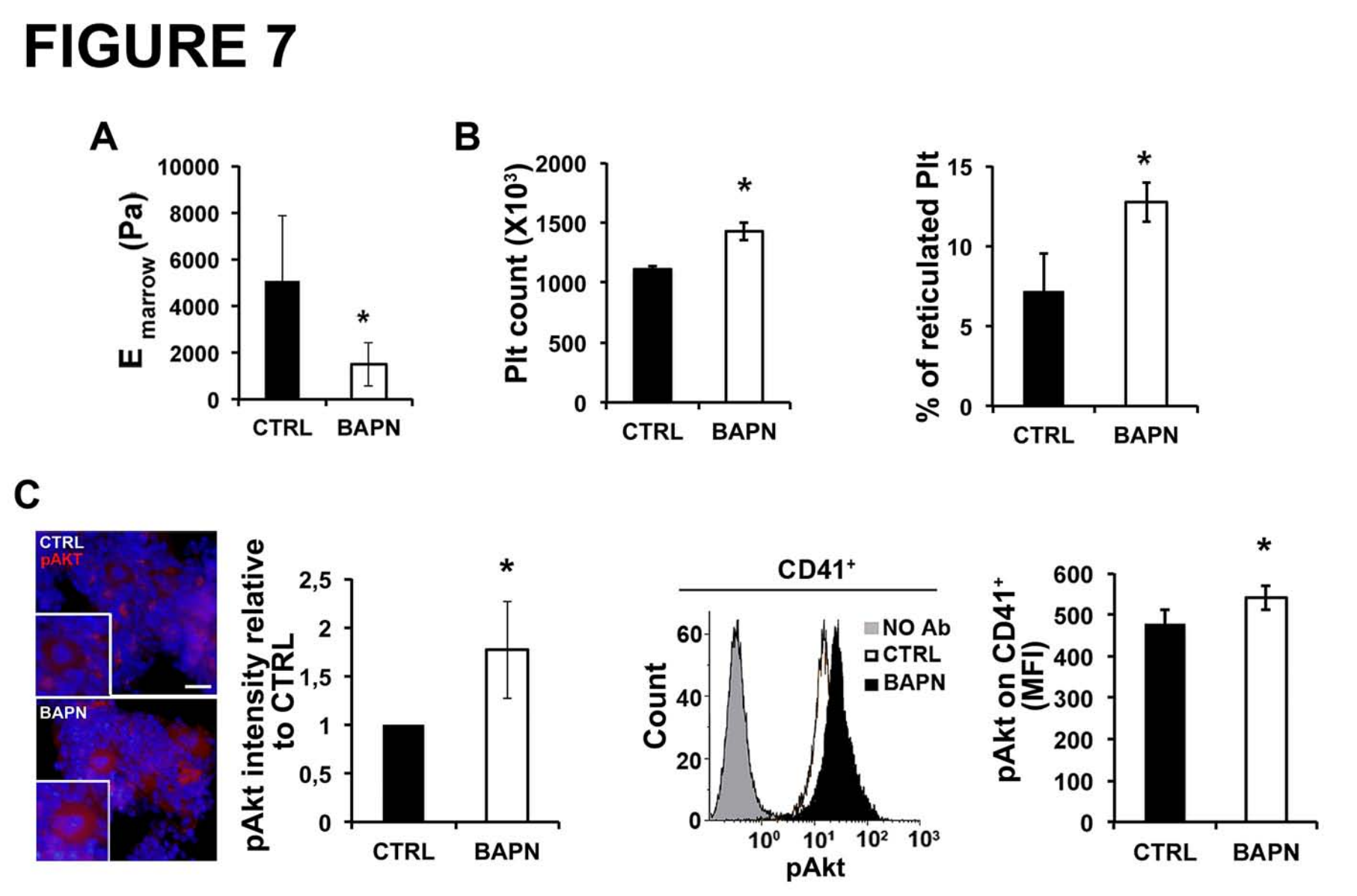
A
B
C
E_{marrow} (Pa)
10000
8000
6000
4000
2000
0
CTRL
BAPN
*
Plt count (X10³)
2000
1500
1000
500
0
% of reticulated Plt
15
10
5
CTRL
pAKT
BAPN
pAkt intensity relative to CTRL
2,5
2
1,5
1
0,5
CD41⁺
NO Ab
CTRL
BAPN
Count
60
40
20
10⁰
10¹
10²
10³
pAkt
pAkt on CD41⁺ (MFI)
600
500
400
300
200
100

FIGURE 8

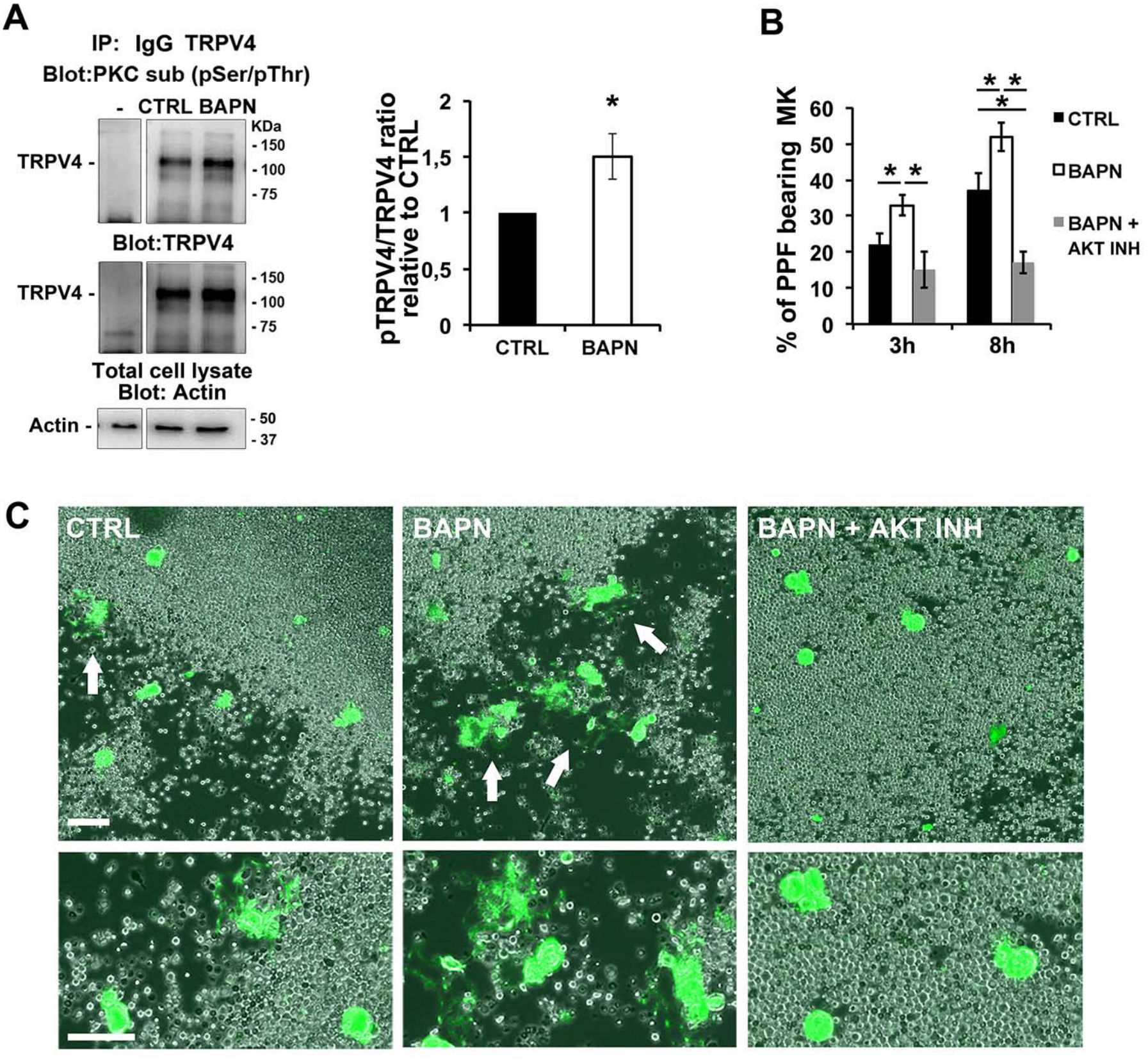
A
IP: IgG TRPV4
Blot:PKC sub (pSer/pThr)
- CTRL BAPN
KDa
TRPV4 -
- 150
- 100
- 75
Blot:TRPV4
TRPV4 -
- 150
- 100
- 75
Total cell lysate
Blot: Actin
Actin -
- 50
- 37
pTRPV4/TRPV4 ratio relative to CTRL
2
1,5
1
0,5
0
*
CTRL
BAPN
B
% of PPF bearing MK
60
50
40
30
20
10
0
* *
* *
*
3h
8h
CTRL
BAPN
BAPN + AKT INH
C
CTRL
BAPN
BAPN + AKT INH

SUPPLEMENTAL MATERIALS AND METHODS

Antibodies

The following antibodies were used: anti- β1 tubulin (kind gift of Prof. J. Italiano Jr); clone HUTS-4, anti-active β1 integrin (Millipore); anti- β1 integrin (Abcam); anti-βActin (Sigma Aldrich); anti-pAKT (ser473; Cell Signaling); anti-Akt (Cell Signaling); anti-pERK (Thr185/Tyr187; Millipore); anti-ERK (Cell Signaling); anti-TRPV4 (Abcam); anti-PE-pAKT (BD Pharmingen); anti-PKC substrates (pSer/pThr; Cell Signaling).

Evaluation of megakaryocyte spreading and proplatelet formation

To analyze Mk spreading and proplatelet formation (PPF) onto collagens, 12 mm glass coverslips or silk films were coated with 25 µg/mL type I (gift of Prof. Maria Enrica Tira; University of Pavia) or type IV collagen (acid soluble) (Sigma Aldrich) overnight at 4°C. At day 13 of differentiation, mature Mks were harvested and allowed to adhere at 37°C and 5% CO_2. To evaluate both the number of spread Mks and PPF, samples were fixed and stained at three well-defined time points, namely at 3, 8 and 16 hours post cell layering on coated surface [1]. These points have been previously shown to be representative of active adhesion (3 hours), starting of PPF (8 hours), and the zenith of PPF and platelet release (16 hours) [2]. The number of spread Mks was assessed as follows: β1 tubulin positive Mks exhibiting stress fibers (stained with TRITC-Phalloidin) were counted and expressed as percentage of spread Mks. PPF were counted as percentage of total Mks.

Immunoprecipitation and Western blotting

Cultured Mks and primary BM immunomagnetically-sorted Mks (CD41+; Biolegend) were collected, washed twice at 4°C and lysed in hepes-glycerol lysis buffer (Hepes 50 mM, 10% glycerol, 1% Triton x-100, $MgCl_2$ 1.5 mM, EGTA 1mM) containing aprotinin 1 µg/mL and leupeptin 1 µg/mL, for 30 min at 4°C, as previously described [3]. After centrifugation at 15700xg for 15' at 4°C, Laemmli sample buffer was added to supernatants. For active β1 integrin staining (clone HUTS-4) samples were not reduced. Samples were then heated at 95 °C for 3' and loaded and run on 8% or 12% sodium dodecyl

sulfate polyacrylamide gel (SDS-PAGE) and transferred to polyvinylidine fluoride membranes (PVDF). Membranes were incubated with 5% BSA, 0.1% Tween in PBS to avoid non specific antibody binding, and then probed with primary antibodies and the appropriate peroxidase conjugated secondary antibodies. Western blots were developed with enhanced chemiluminescence reagents and Chemidoc XRS Imaging System (BioRad). For immunoprecipitation, cellular lysates were precleared by incubation with protein A-Sepharose. Precleared lysates were incubated with 2 µg of anti-TRPV4 antibody (4 µg/mL; Abcam) for 4 h at 4°C on a rotatory shaker, followed by adding 100 µL of 50 mg/ml protein A-Sepharose and incubation overnight at 4°C on a rotatory shaker. Beads were washed three times in lysis buffer.

Immunofluorescence microscopy

The cover-slips were mounted onto glass slides with ProLong Gold antifade reagent (Invitrogen). For immunofluorescence staining of BM samples, sections were fixed for 20 minutes in 4% PFA, washed with PBS, and blocked with 2% bovine serum albumin (BSA) (Sigma-Aldrich) in PBS for 30 minutes. Non-specific binding sites were saturated with a solution of 5% goat serum, 2% BSA, and 0.1% glycine in PBS for 1 hour. Specimens were incubated with primary antibodies in washing buffer (0.2% BSA, 0.1% Tween in PBS) overnight at 4°C. After three washes, sections were incubated with appropriate fluorescently conjugated secondary antibodies in washing buffer for 1 hour at room temperature (RT). Nuclei were counterstained using Hoechst 33258 (100 ng/mL in PBS) at RT for 3 minutes. Sections were then mounted with micro-cover glass slips using Fluoro-mount (Bio-Optica). Negative controls were routinely included by omitting the primary antibodies.

Internalization assays

For immunofluorescence internalization assay, Mks were washed in RPMI medium (Euroclone) containing 0.1% BSA and pre-cooled on ice before treatment with 15 µg/ml of anti-β1 integrin antibody (Abcam) ($1x10^5$ cells in 100 µl RPMI, 0.1% BSA with mAb) for 30 minutes on ice with gentle agitation. After washing with ice-cold RPMI, 0.1% BSA to remove unbound antibody,

cells were seeded on type I or type IV collagen-coated coverslips, or on type I collagen coated soft and stiff silk films for 3 hour at 37°C. Before fixation, cells were placed on ice and acid washed (three washes with ice-cold 50 mM glycine in Ca2+/Mg2+ HBSS, pH 2.5, and two washes with Ca2+/Mg2+ HBSS, pH 7.5) to remove the antibody from the cell surface. Mks were then fixed, permeabilized, and stained with the appropriate secondary antibody as described in the "immunofluorescence microscopy" section [4].

For western blotting internalization assay, Mks at day 13 of culture ($1.5x10^6$) were cooled on ice and washed in pre-chilled PBS before incubation with PBS 0.5 mg/mL thiol-cleavable Sulfo-NHS-S-S-Biotin (Pierce Chemical Co.) for 1 hour on ice. After washing with ice-cold PBS, labeled Mks were resuspended in serum-free RPMI medium and plated on the indicated substrates for the indicated time points at 37°C to allow β1 integrin internalization. After plating Mks for indicated times, samples were returned to ice, washed three times with ice-cold PBS, and treated with two successive reductions of 20 minutes with a reducing solution containing the non-membrane permeable reducing agent glutathione (GSH; 42 mM), 75 mM NaCl, 1 mM EDTA, 1% bovine serum albumin and 75 mM NaOH. To evaluate total labeling, a sample was not reduced with GSH.

Silk solution preparation

Silk fibroin aqueous solution was obtained from Bombyx mori silkworm cocoons according to previously published literature [5-7]. Briefly, Bombyx mori cocoons were de-wormed and chopped. 5 g of chopped cocoons were boiled for 10 minutes in 2 L of 0.02 M Na_2CO_3 solution. Resulting fibers were rinsed for three times in distilled water and dried overnight. The dried fibers were solubilized for 4 hours at 60°C in 9.3 M LiBr at a weight to volume ratio of 3 g/12 mL. The solubilized silk solution was dialyzed against distilled water using a Slide-A-Lyzer cassette (Thermo Scientific) with a 3,500 MW cutoff for three days. Water was changed a total of eight times. The silk solution was centrifuged at 3220xg for 10 minutes to remove large particulates and stored at 4°C.

Silk film fabrication and assembly of the transwell chamber system

Silk solution (1% w/v), was cast on 6 well plates (45 μL/cm^2 of surface area) and dried at 22°C for 16 hours. Silk films were water annealed in a vacuum chamber, containing 100 mL of water at the bottom of chamber, for stiffness tuning. The water annealing chamber was maintained at either 60°C for 16 hours or 4°C for 6 hours to achieve stiff or soft silk film mechanical properties, respectively. Before Mk plating, silk films were exposed to ultraviolet light for 30 minutes per side inside of a sterile biological hood. For immunofluorescence experiments, films were cast on polydimethylsiloxane (PDMS) mold and dried at 22°C for 16 hours. Silk films were lift off the PDMS mold and water annealed as described in the text. Successively, silk films were secured between two rings of scotch tape (6 mm inner diameter, 12 mm outer diameter) and secured to the bottom of a 24-well plates using silicon rings (10 mm inner diameter, 15.5 mm outer diameter, McMaster Carr). All samples were sterilely washed three times in PBS over the course of 24 hours. The transwell chamber system for the analysis of platelet production was assembled as previously described [8]. Briefly, silk solution (1% w/v) was mixed with polyethylene oxide (PEO) porogen (0.05% w/v; Sigma) before casting on the PDMS mold, dried and water annealed in order to obtain porous silk films of different stiffness. The membrane from transwell inserts (Corning) was then removed under sterile conditions using a biopsy punch. Porous silk films were trimmed using an 8 mm diameter biopsy punch and secured to the transwell insert using a sterile, medical-grade silicon glue (Dow Corning). The films were rinsed three times in PBS over the course of 24 hours to remove the PEO porogen. In all experiments, silk films were soaked in cell culture media for one hour, prior to cell seeding.

Elastic modulus determination via Atomic Force Microscope

Elastic modulus maps were taken on an Asylum Research MFP-3D Atomic Force Microscope (AFM) (Asylum Research) using AC240TS-R3 cantilevers (Asylum Research) with a nominal spring constant of 2 N/m. Films were hydrated with PBS and a minimum of 300 AFM force vs. indentation curves were taken in the fluid solution on each film. Cantilevers were calibrated in air and in the buffer solution prior to measurement to determine accurate spring constant values. Elastic modulus values were determined using the inbuilt

Hertz Model fitting function of the Asylum Research MFP3D software [9]. To analyze collagen structures in different conditions, type I and type IV were coated on silk films cast on glass coverslips as described in “Silk film fabrication” and then observed by tapping-mode atomic force microscopy on a Digital Instruments multimode Nano- Scope III/a SPM (Digital Instruments) with Olympus OTR 8 oxide-sharpened silicon nitride probes [3].

Reverse transcription (RT)-PCR and quantitative Real Time PCR

In vitro differentiated Mks at day 13 of culture were purified using immunomagnetic beads technique [9]. Total RNA was extracted using the Mammalian GeneElute total RNA kit (Sigma-Aldrich). Retrotrascription (RT) was performed using the iScriptTM cDNA Synthesis Kit according to the manufacturer instructions (BioRad). RT-PCR was performed as previously described [3]. For quantitative Real Time PCR, RT samples were diluted up to three times with ddH_2O and the resulting cDNA was amplified in triplicate with 200 nM of primers and SsoFast Evagreen Supermix (BioRad). The amplification was performed in a CFX Real-time system (BioRad) as follows 95°C for 5’, 35 cycles at 95°C for 10’’, 60°C for 15’’, 72°C for 20’’. Pre-designed KiCqStart primers were purchased from Sigma Aldrich (Milan, Italy). The BioRad CFX Manager software 3.0 was used for the normalization of the samples (BioRad). β -2 microglobulin gene expression was used for comparative quantitative analysis.

Elastic modulus determination via Atomic Force Microscope

Elastic modulus maps were taken on an Asylum Research MFP-3D Atomic Force Microscope (AFM) (Asylum Research) using AC240TS-R3 cantilevers (Asylum Research) with a nominal spring constant of 2 N/m. Films were hydrated with PBS and a minimum of 300 AFM force vs. indentation curves were taken in the fluid solution on each film. Cantilevers were calibrated in air and in the buffer solution prior to measurement to determine accurate spring constant values. Elastic modulus values were determined using the inbuilt Hertz Model fitting function of the Asylum Research MFP3D software [9].

[Ca^{2+}]i measurements

PSS consists of: NaCl 150 mM, KCl 6 mM, CaCl2 1.5 mM, MgCl2 1 mM, glucose 10 mM, Hepes 10 mM. In Ca2+-free solution (0Ca2+), Ca2+ was substituted with NaCl 2 mM and EGTA 0.5 mM was added. Solutions were titrated to pH 7.4 with NaOH. After washing in PSS, the coverslip was fixed to the bottom of a Petri dish and the cells were observed using an upright epifluorescence Axiolab microscope (Carl Zeiss), usually equipped with a Zeiss X63 Achroplan objective (water-immersion, 2.0mm working distance, 0.9 numerical aperture). Mks were excited alternately at 340 and 380 nm, and the emitted light was detected at 510 nm. See Supplemental methods. A first neutral density filter (1 or 0.3 optical density) reduced the overall intensity of the excitation light and a second neutral density filter (0.3 optical density) was coupled to the 380 nm filter to approach the intensity of the 340 nm light. A round diaphragm was used to increase the contrast. The excitation filters were mounted on a filter wheel (Lambda 10; Sutter Instrument). Custom software, working in the LINUX environment, was used to drive the camera (Extended-ISIS Camera; Photonic Science) and the filter wheel and to measure and plot on-line the fluorescence from 10 to 15 rectangular regions of interest (ROI) enclosing 10-15 single cells. [Ca^{2+}]i was monitored by measuring, for each ROI, the ratio of the mean fluorescence emitted at 510 nm when exciting alternatively at 340 and 380nm (shortly termed ‘‘ratio’’). An increase in [Ca^{2+}]i causes an increase in the ratio [2].

Animals and *in vivo* treatment

For in vivo BAPN treatment, mice were injected with 350 mg/Kg/day of BAPN (Sigma Aldrich) and were given drinking water containing 0.2% (w/v) BAPN for 14 days. At day 14 after the first injection, mice were sacrificed and blood was collected for peripheral blood count. Femurs were fixed in 3% PFA or alternatively flushed and used for flow cytometry analysis, BM explants and Mk cell sorting experiments. Age- and sex-paired mice (10-12 weeks-old males) were injected with PBS as control. Cell count and differential cell count in blood samples were performed on an ADVIA 120 hematology analyzer (Siemens).

In vivo bone marrow stiffness

Samples were subjected to cyclic uniaxial compression test with a strain rate of 0.01 s^{-1}, up to 4% deformation, at room temperature and in wet condition. Before testing, samples were preserved in PBS, and their length and cross sectional area were measured with a caliper (10 μm resolution). The compressive elastic modulus of each sample was evaluated from the slope of the first linear portion of the stress–strain curve [10].

Flow cytometry

All samples were acquired with a Beckman Coulter FacsDiva flow cytometer (Beckman Coulter Inc.). The analytical gating were set using unstained samples and relative isotype controls. Off line data were analyzed using Beckman Coulter Kaluza version software package (Beckman Coulter Inc.).

Bone marrow explants

Intact bone marrows were obtained by flushing mouse femurs with PBS buffer. Ten 0.5 mm thick transversal sections from one femur from the same mouse were placed at 37°C in an incubation chamber containing DMEM medium supplemented with 5% mouse serum. Living tissue sections were examined by phase contrast under an inverted microscope (Olympus IX53). Images for video were acquired sequentially at 8-minutes intervals with Olympus FluoView FV10i and processed with FV10 ASW 4.0 software (Olympus). Mks were stained as living cells with anti-CD41-FITC antibody (0.001mg/mL; Biolegend) making them visible and recognizable within the explants. Mks were classified as proplatelet forming cells when at least one thin extension presenting a proplatelet bud was observed. To perform TRPV4 immunoprecipitation in Mks from BM explants, Mks were sorted by immunostaining with a phycoerythrin (PE)-conjugated anti-mouse CD41 (0.1 mg/mL; Biolegend) followed by incubation with anti-PE immunomagnetic beads (Miltenyi biotech). The purity of isolated Mks, by means of CD42b and CD61 staining, were routinely analyzed.

Tissue collection and immunohistochemistry

Femurs from treated and control animals were removed and fixed for 24 hours in 3% paraformaldehyde (PFA). Bones were decalcified in a solution of 10% EDTA in PBS (w/o calcium and magnesium) pH 7.2, for 2 weeks at 4°C. Bones were embedded in OCT cryosectioning medium and snap frozen in a chilling bath. 8 µm tissue sections were taken using a Microm Microtome HM 250 (Bio Optica S.P.A.) and stained with anti-CD41 (0.1 mg/mL in PBS/1%BSA/0.3% Triton X-100; Biolegend) and anti-pAkt (diluted 1:25 in PBS/1%BSA/0.3% Triton X-100; Cell signaling) and the appropriate secondary antibodies for fluorescence microscopy analysis [7].

Reticulated platelet analysis

To assess platelet production *in vivo*, a small sample of blood was collected from the tail vein and placed in anticoagulant. The blood was then diluted 20x in 2 mM EDTA in PBS before the addition of 100 ng/mL thiazole orange (Sigma Aldrich) for 60 minutes at room temperature to label reticulated platelets. The samples were then fixed in 1% PFA for 15 minutes and analyzed by flow cytometry. Thiazole orange-positive/$CD41^+$ platelets were considered reticulated [11].

Lox-mediated collagen crosslinking

Recombinant LOXL2 was purchased by R&D systems (2369-AO). Acid soluble type IV collagen (25 µg/mL; Sigma Aldich) was coated on 96-well plates alone or in combination with 4µg/mL of LOXL2 recombinant protein, or in combination with 4µg/mL of LOXL2 recombinant protein plus 200 µM BAPN, overnight at 4°C, following by incubation at 37°C for 24 hours and by three washes with PBS, prior to cell plating [12,13]. After 16 hours, non-adherent cells were removed and adhering Mks were fixed with 4% PFA. Proplatelet forming Mks were counted and expressed as percentage of proplatelet bearing Mks, using protocols we previously employed [1].

Statistics

Values are expressed as mean ± SD. *t test* was used to analyze experiments. A value of $p<0.05$ was considered statistically significant. All experiments were independently repeated at least three times.

REFERENCES

1. Balduini A, Pallotta I, Malara A, et al. Adhesive receptors, extracellular proteins and myosin IIA orchestrate proplatelet formation by human megakaryocytes. J Thromb Haemost. 2008;6(11):1900-1907.
2. Di Buduo CA, Moccia F, Battiston M, et al. The importance of calcium in the regulation of megakaryocyte function. Haematologica. 2014;99(4):769-778.
3. Abbonante V, Gruppi C, Rubel D, Gross O, Moratti R, Balduini A. Discoidin domain receptor 1 protein is a novel modulator of megakaryocyte-collagen interactions. J Biol Chem. 2013;288(23):16738-16746.
4. Cera MR, Fabbri M, Molendini C, et al. JAM-A promotes neutrophil chemotaxis by controlling integrin internalization and recycling. J Cell Sci. 2009;122(Pt 2):268-277.
5. Zahr AA, Salama ME, Carreau N, et al. Bone marrow fibrosis in myelofibrosis: pathogenesis, prognosis and targeted strategies. Haematologica. 2016;101(6):660-671.
6. Deng J, Liu Y, Lee H, et al. S1PR1-STAT3 signaling is crucial for myeloid cell colonization at future metastatic sites. Cancer Cell. 2012;21(5):642-654.
7. Malara A, Currao M, Gruppi C, et al. Megakaryocytes contribute to the bone marrow-matrix environment by expressing fibronectin, type IV collagen, and laminin. Stem Cells. 2014;32(4):926-937.
8. Di Buduo CA, Wray LS, Tozzi L, et al. Programmable 3D silk bone marrow niche for platelet generation ex vivo and modeling of megakaryopoiesis pathologies. Blood. 2015;125(14):2254-2264.
9. Malara A, Gruppi C, Pallotta I, et al. Extracellular matrix structure and nano-mechanics determine megakaryocyte function. Blood. 2011;118(16):4449-4453.
10. Urciuolo A, Quarta M, Morbidoni V, et al. Collagen VI regulates satellite cell self-renewal and muscle regeneration. Nat Commun. 2013;4:1964.
11. Mason KD, Carpinelli MR, Fletcher JI, et al. Programmed anuclear cell death delimits platelet life span. Cell. 2007;128(6):1173-1186.
12. Cox TR, Bird D, Baker AM, et al. LOX-mediated collagen crosslinking is responsible for fibrosis-enhanced metastasis. Cancer Res. 2013;73(6):1721-1732.
13. Rodriguez HM, Vaysberg M, Mikels A, et al. Modulation of lysyl oxidase-like 2 enzymatic activity by an allosteric antibody inhibitor. J Biol Chem. 2010;285(27):20964-20974.

SUPPLEMENTAL FIGURES AND FIGURE LEGENDS

SUPPLEMENTAL FIGURE 1

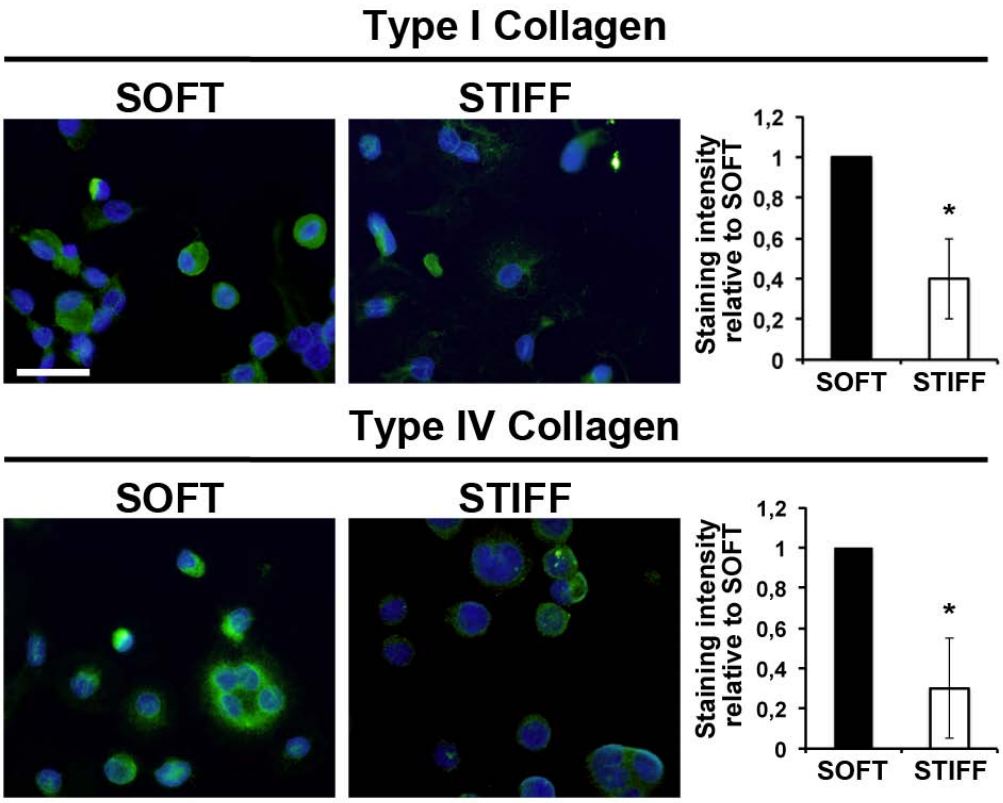

SUPPLEMENTAL FIGURE 1. A) Representative images of active beta 1 integrin immunofluorescence staining in human mature Mks plated, for 3 hours, on type I collagen or type IV collagen coated soft or stiff silk fibroin films. Staining intensities were quantified by ImageJ software. n = 100 Mks per experimental condition in at least three independent experiments. Staining intensities are expressed relative to soft. * $p < 0.05$

SUPPLEMENTAL FIGURE 2

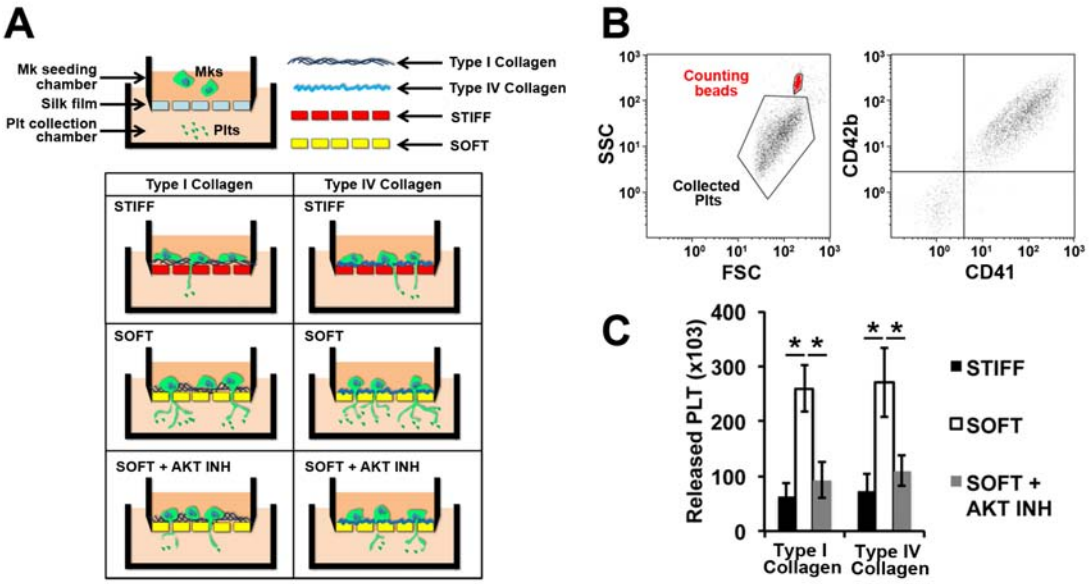

SUPPLEMENTAL FIGURE 2. A) Schematic representation of the transwell system for platelet (Plts) production. B) Representative flow cytometry dot plot of platelets collected in the lower chamber of the system. Platelets were stained with anti-CD41 and anti-CD42b antibodies and counted with bead standard. C) Number of $CD41^{+}/CD42b^{+}$ platelets in the different experimental conditions. n = 3 per experimental condition.

SUPPLEMENTAL FIGURE 3

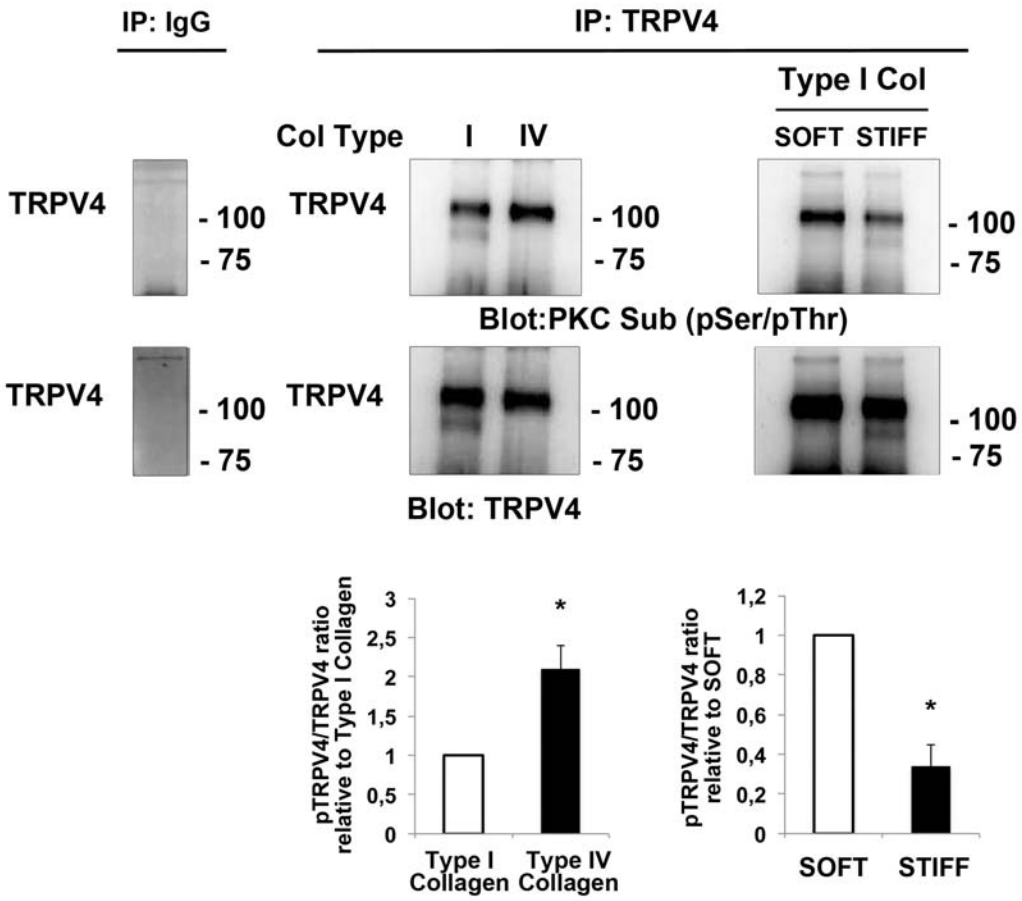

SUPPLEMENTAL FIGURE 3. A) Western blot analysis of phosphorylated TRPV4 in Mks plated for 3 hours on type I and type IV collagen. Mk were lysed and TRPV4 immunoprecipitated with anti TRPV4 antibody. Membranes were probed with anti-PKC substrates antibody and re-probed with anti-TRPV4 antibody to show the equal loading. B) Western blot analysis of phosphorylated TRPV4 in Mks plated for 3 hours on type I collagen coated SOFT or STIFF silk films. Mk were lysed and TRPV4 immunoprecipitated with anti TRPV4 antibody. Membranes were probed with anti-PKC substrates antibody and re-probed with anti-TRPV4 antibody to show the equal loading. A control sample was immunoprecipitated with an unrelated antibody (IgG). C) Densitometry analysis of the western blot in A and B. Data are expressed as mean ± SD for three independent experiments per each class of experiments. * $p<0.05$.

SUPPLEMENTAL FIGURE 4

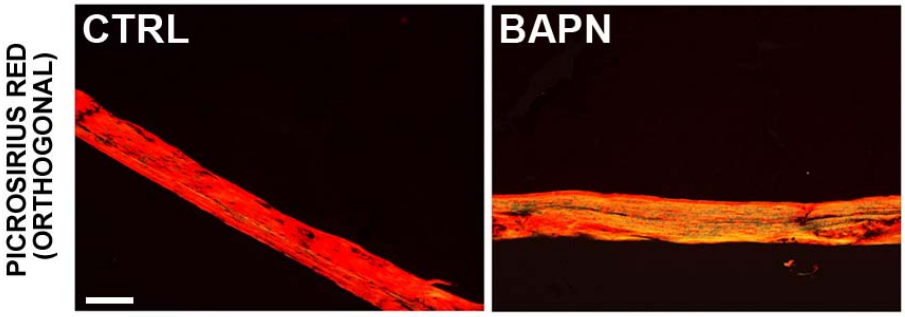

SUPPLEMENTAL FIGURE 4. A) Photomicrographs of CTRL and BAPN treated mouse femurs stained with picrosirius red, viewed under an orthogonal polarizing filters. Scale bar 100 μm.

SUPPLEMENTAL FIGURE 5

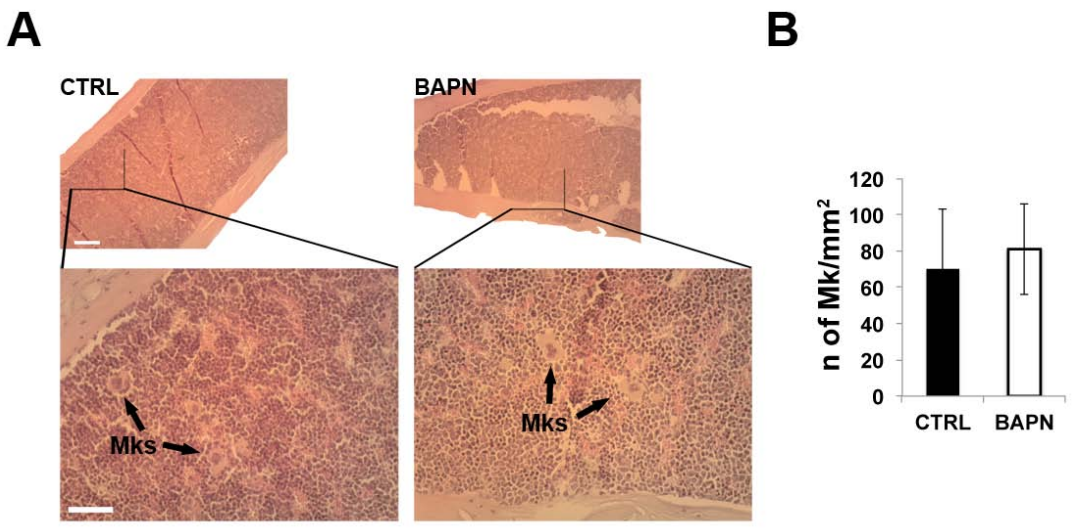

SUPPLEMENTAL FIGURE 5. A) Photomicrographs of CTRL and BAPN treated mouse femurs stained with Hematoxylin and Eosin. Bone marrow Mks are clearly visible (arrows). B) Bone marrow Mks were counted and expressed as number of Mks per mm^2. Data are expressed as mean ± SD (n=4).

SUPPLEMENTAL FIGURE 6

A

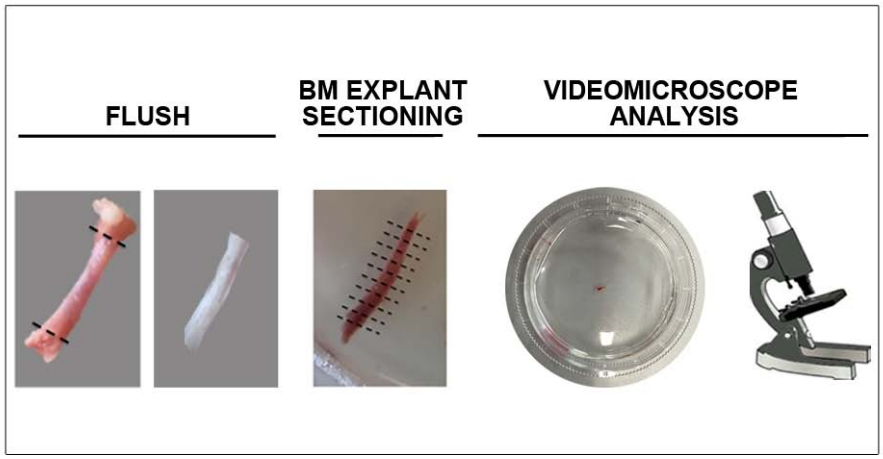

B

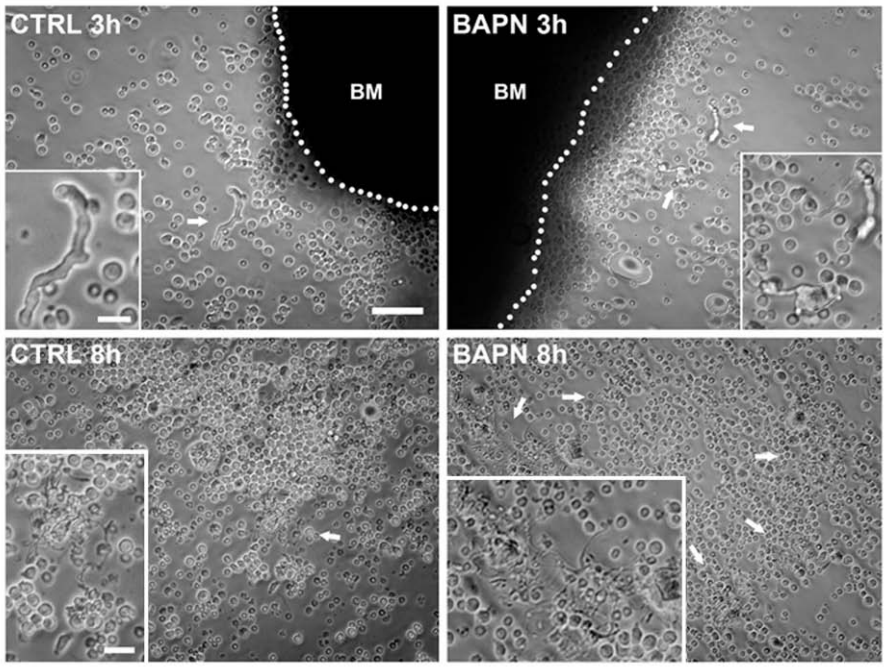

SUPPLEMENTAL FIGURE 6. A) Flow chart of the bone marrow explant experiments. B) Phase contrast photomicrographs of CTRL and BAPN treated bone marrow explants after 3 and 8 hours from the beginning of the experiments. Proplatelet extending Mks are visible (arrows). Scale bar 50 μm (box scale bar 10 μm). BM (bone marrow).

SUPPLEMENTAL FIGURE 7

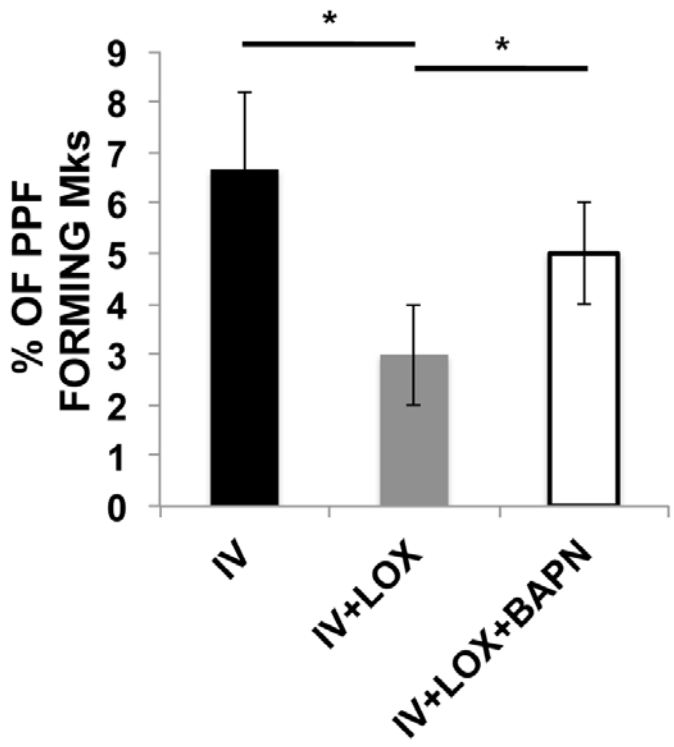

SUPPLEMENTAL FIGURE 7. Mature Mks were plated for 16 hours on 96-well plates coated with 25 μg/mL type IV collagen alone, type IV collagen pre-treated overnight with 4μg/mL LOXL2, or type IV collagen pre-treated with 4μg/mL LOXL2 + 200 μM BAPN overnight, as detailed under Methods. After 16 hours of adherence cells were fixed and counted for proplatelet formation. Data are expressed as mean ± SD (n=5) * $p<0.05$.

SUPPLEMENTAL TABLE 1

TEST	CTRL (mean±SD)	BAPN (mean±SD)	P VALUE
WBC	3,03±1,12	2,76±1,25	n.s.
RBC	10,26±1,76	8,01±1,72	n.s.
PDW	51,58±8,26	81,18±4,63	p < .01
MPV	7,17±0,82	10,1±1,77	p < .01

SUPPLEMENTAL TABLE 1.

Blood cell count in CTRL and BAPN treated mice. Data refer to ten mice per group.

Supplemental Video 1. Videoclip of Mks extending proplatelets in bone marrow explants from CTRL mice. After bone marrow explant, Mks were stained as living cells with anti-CD41-FITC antibody. Images were acquired sequentially (1 frame/8 minutes) and the movie was accelerated to 1 frame/400 milliseconds. Total real duration: 160 min. An average of one Mk extending proplatelets per field is visible.

Supplemental Video 2. Videoclip of Mks extending proplatelets in bone marrow explants from BAPN treated mice. After bone marrow explant, Mks were stained as living cells with anti-CD41-FITC antibody. Images were acquired sequentially (1 frame/8 minutes) and the movie was accelerated to 1 frame/400 milliseconds. Total real duration: 160 min. An average of three Mks extending proplatelets per field is visible.

Supplemental Video 3. Videoclip of Mks extending proplatelets in bone marrow explants from BAPN treated mice treated with an Akt inhibitor. After bone marrow explant, Mks were stained as living cells with anti-CD41-FITC antibody. Images were acquired sequentially (1 frame/8 minutes) and the movie was accelerated to 1 frame/400 milliseconds. Total real duration: 160 min. Mks present a significantly decreased ability to extend proplatelets.